APLP2 Regulates Refractive Error and Myopia Development in Mice and Humans

Andrei V. Tkatchenko[1,2☯*], **Tatiana V. Tkatchenko**[1☯], **Jeremy A. Guggenheim**[3☯], **Virginie J. M. Verhoeven**[4,5], **Pirro G. Hysi**[6], **Robert Wojciechowski**[7,8], **Pawan Kumar Singh**[9], **Ashok Kumar**[9,10], **Gopal Thinakaran**[11], **Consortium for Refractive Error and Myopia (CREAM)**[¶], **Cathy Williams**[12]

1 Department of Ophthalmology, Columbia University, New York, New York, United States of America, **2** Department of Pathology and Cell Biology, Columbia University, New York, New York, United States of America, **3** School of Optometry & Vision Sciences, Cardiff University, Cardiff, United Kingdom, **4** Department of Ophthalmology, Erasmus Medical Center, Rotterdam, Netherlands, **5** Department of Epidemiology, Erasmus Medical Center, Rotterdam, Netherlands, **6** Department of Twin Research and Genetic Epidemiology, King's College London School of Medicine, London, United Kingdom, **7** Department of Epidemiology, Johns Hopkins Bloomberg School of Public Health, Baltimore, Maryland, United States of America, **8** Statistical Genetics Section, Inherited Disease Research Branch, National Human Genome Research Institute (NIH), Baltimore, Maryland, United States of America, **9** Department of Ophthalmology, Wayne State University, Detroit, Michigan, United States of America, **10** Department of Anatomy and Cell Biology, Wayne State University, Detroit, Michigan, United States of America, **11** Departments of Neurobiology, Neurology, and Pathology, University of Chicago, Chicago, Illinois, United States of America, **12** School of Social and Community Medicine, University of Bristol, Bristol, United Kingdom

☯ These authors contributed equally to this work.
¶ A full list of CREAM members and their affiliations appears in the Supporting Information.
* avt2130@cumc.columbia.edu

OPEN ACCESS

Abstract

Myopia is the most common vision disorder and the leading cause of visual impairment worldwide. However, gene variants identified to date explain less than 10% of the variance in refractive error, leaving the majority of heritability unexplained ("missing heritability"). Previously, we reported that expression of *APLP2* was strongly associated with myopia in a primate model. Here, we found that low-frequency variants near the 5'-end of *APLP2* were associated with refractive error in a prospective UK birth cohort (n = 3,819 children; top SNP rs188663068, $p = 5.0 \times 10^{-4}$) and a CREAM consortium panel (n = 45,756 adults; top SNP rs7127037, $p = 6.6 \times 10^{-3}$). These variants showed evidence of differential effect on childhood longitudinal refractive error trajectories depending on time spent reading (gene x time spent reading x age interaction, $p = 4.0 \times 10^{-3}$). Furthermore, *Aplp2* knockout mice developed high degrees of hyperopia ($+11.5 \pm 2.2$ D, $p < 1.0 \times 10^{-4}$) compared to both heterozygous (-0.8 ± 2.0 D, $p < 1.0 \times 10^{-4}$) and wild-type ($+0.3 \pm 2.2$ D, $p < 1.0 \times 10^{-4}$) littermates and exhibited a dose-dependent reduction in susceptibility to environmentally induced myopia ($F_{(2, 33)} = 191.0$, $p < 1.0 \times 10^{-4}$). This phenotype was associated with reduced contrast sensitivity ($F_{(12, 120)} = 3.6$, $p = 1.5 \times 10^{-4}$) and changes in the electrophysiological properties of retinal amacrine cells, which expressed *Aplp2*. This work identifies *APLP2* as one of the "missing" myopia genes, demonstrating the importance of a low-frequency gene variant in the development of human myopia. It also demonstrates an important role for *APLP2* in

refractive development in mice and humans, suggesting a high level of evolutionary conservation of the signaling pathways underlying refractive eye development.

Author Summary

Gene variants identified by GWAS studies to date explain only a small fraction of myopia cases because myopia represents a complex disorder thought to be controlled by dozens or even hundreds of genes. The majority of genetic variants underlying myopia seems to be of small effect and/or low frequency, which makes them difficult to identify using classical genetic approaches, such as GWAS, alone. Here, we combined gene expression profiling in a monkey model of myopia, human GWAS, and a gene-targeted mouse model of myopia to identify one of the "missing" myopia genes, *APLP2*. We found that a low-frequency risk allele of *APLP2* confers susceptibility to myopia only in children exposed to large amounts of daily reading, thus, providing an experimental example of the long-hypothesized gene-environment interaction between nearwork and genes underlying myopia. Functional analysis of *APLP2* using an *APLP2* knockout mouse model confirmed functional significance of *APLP2* in refractive development and implicated a potential role of synaptic transmission at the level of glycinergic amacrine cells of the retina for the development of myopia. Furthermore, mouse studies revealed that lack of *Aplp2* has a dose-dependent suppressive effect on susceptibility to form-deprivation myopia, providing a potential gene-specific target for therapeutic intervention to treat myopia.

Introduction

Postnatal refractive eye development is a tightly coordinated process whereby visual experience fine-tunes a genetic program of ocular growth towards an optimal match between the optical power of the eye and its axial length in a process called "emmetropization" [1,2]. The emmetropization process is regulated by a vision-driven feedback loop in the retina and downstream signaling cascades in other ocular tissues, and normally results in sharp vision (emmetropia). Failure to achieve or maintain emmetropia leads to the development of refractive errors, i.e., farsightedness (hyperopia) or nearsightedness (myopia). Myopia is the most common vision disorder worldwide [3]. The prevalence of myopia has increased from 25% to 44% of the adult population in the United States in the last 30 years [4], and reached more than 80% of young adults in some parts of Asia [5,6]. Myopia negatively affects self-perception, job/activity choices, and ocular health [7–9]. Epidemiological data suggest that common myopia represents a major risk factor for a number of potentially blinding ocular diseases such as cataract, glaucoma, retinal detachment, and myopic maculopathy, which is comparable to the risks associated with hypertension for stroke and myocardial infarction, and represents one of the leading causes of blindness [10–12]. It is estimated that 2.5 billion people (1/3 of the world's population) will be affected by myopia by 2020 [13]. Uncorrected refractive errors are the major cause of vision loss and refractive errors and is one of five World Health Organization's designated priority health conditions [3,13].

Refractive eye development is controlled by both environmental and genetic factors [14–17]. However, genetic factors are believed to play a key role in determining the impact of environmental factors on refractive eye development, including populations that have experienced rapid rises in the prevalence of myopia in recent decades [14–18]. Human population studies
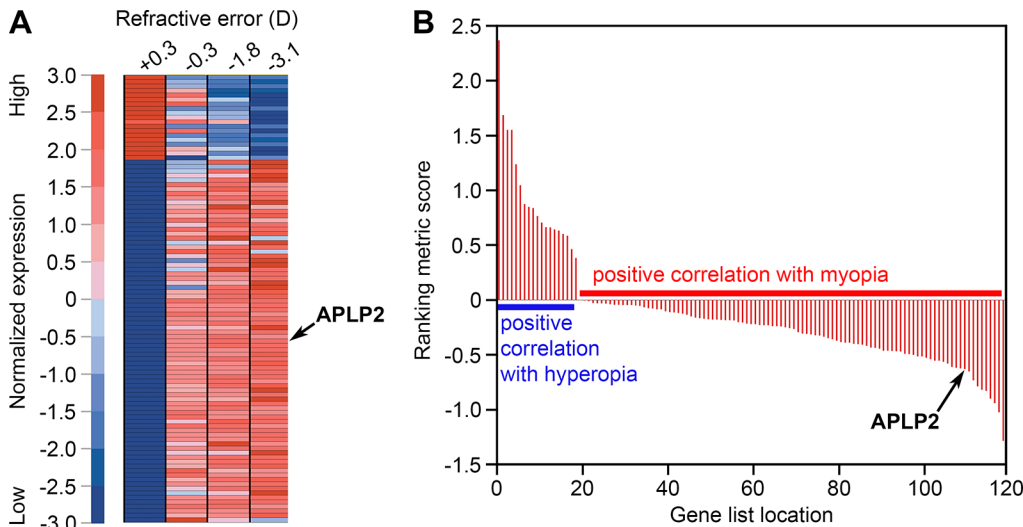
Fig 1. *APLP2* expression is associated with myopic phenotype in the monkey model of myopia. (**A**) Gene set enrichment analysis (GSEA) identified genes differentially expressed in the retina of monkeys with refractive errors induced by form-deprivation. Expression patterns of these genes exhibited statistically significant associations with phenotype "myopia" versus "hyperopia". The heat map shows genes with the highest positive correlation with either the myopic or hyperopic phenotype. The expression level for each gene was normalized across the samples such that the mean was 0 and the standard deviation (SD) was 3. Expression levels greater than the mean are shaded in red, and those bellow the mean are shaded in blue. The scale (left) indicates SDs above or below the mean. (**B**) Graph showing the distribution of the GSEA correlation (ranking metric) scores for the 119 differentially expressed genes. Ranking metric score reflects the strength of correlation between a gene's expression pattern and either the myopic or hyperopic phenotype. Positive values indicate a positive correlation with hyperopia and a negative correlation with myopia (i.e., downregulation in myopia and overexpression in hyperopia). Negative values indicate a positive correlation with myopia and a negative correlation with hyperopia (i.e., overexpression in myopia and downregulation in hyperopia). Arrows identify *APLP2*, which was found to be overexpressed in myopia, suppressed in hyperopia, had strong positive association with myopic phenotype and was negatively correlated with hyperopia (ranking metric score -0.63). These analyses were carried out using gene expression data previously reported by Tkatchenko et al. [53].

suggest that contribution of genetic factors accounts for 60%-90% of variance in refraction [19–24]. Human genetic mapping studies have identified over 24 chromosomal loci linked to myopia [15,25–30]. However, the currently-identified variants account for only a small fraction of myopia cases [31] suggesting the existence of a large number of yet unidentified low-frequency or small-effect variants, which underlie the majority of myopia cases [32–35]. Here, we present genetic and functional evidence identifying amyloid beta (A4) precursor-like protein 2 (*APLP2*), which was previously found to be involved in synaptic plasticity and transmission in the central nervous system [36–52], as one such myopia-susceptibility gene.

Results

Genetic variation at the *APLP2* locus is associated with myopia in children and adults

In a previous study designed to identify genes differentially expressed in myopic eyes, we performed large-scale gene expression profiling in the retina of green monkeys (*Chlorocebus aethiops*) with experimentally induced myopia and identified 119 differentially expressed genes [53]. Here, gene set enrichment analysis (GSEA) [54,55] of these data revealed that expression of one of these genes, *APLP2*, among others was strongly associated with the refractive error phenotype. *APLP2* was found to be overexpressed in myopia and suppressed in hyperopia (Fig 1 and S1 Table).

To explore whether genetic variants within or nearby *APLP2* influence refractive error development in humans, single nucleotide polymorphism (SNP) genetic variants within
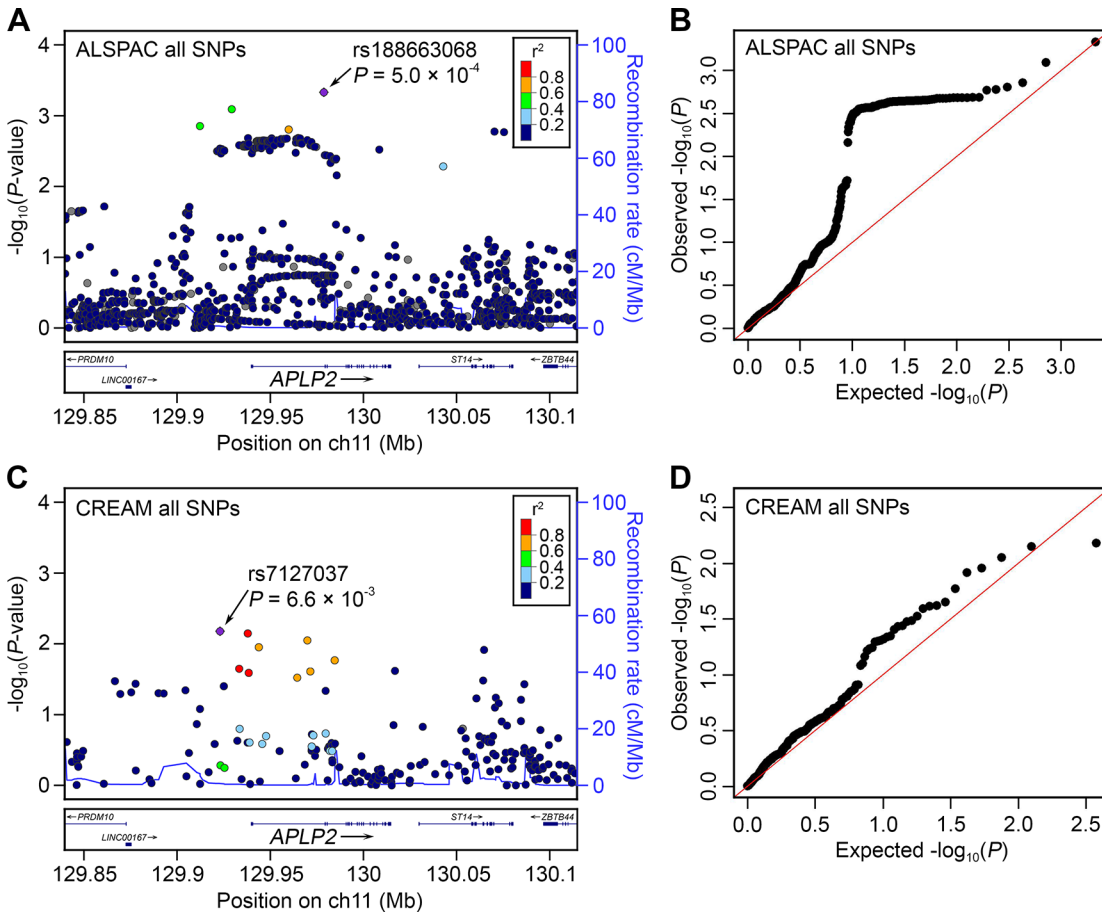
Fig 2. Association between genetic variants at the *APLP2* locus and refractive error in children and adults. The y-axis of all graphs indicates the observed $\log_{10}$ (P-values) for single-marker association tests from GWAS for refractive error, for SNPs within 100 kb of the *APLP2* gene in children (n = 3,819) participating in the ALSPAC study (**A, B**) and adults (n = 45,756) participating in the CREAM consortium sample (**C, D**). Region plots for all SNPs examined (**A, C**) show genomic position on the x-axis (build hg19 coordinates) while the colour coding indicates LD (r^2) with the lead SNP estimated from CEU individuals in HapMap Phase 2, and the right-hand y-axis indicates the recombination rate. Quantile-quantile plots (**B, D**) display expected $\log_{10}$ (P-values) on the x-axis.

100 kb of the *APLP2* gene were tested for association with refractive error in children participating in a UK birth cohort study (the Avon Longitudinal Study of Parents and Children, ALSPAC). Numerous SNPs in an LD block that encompassed the promoter region and 5'-end of the *APLP2* gene were associated with refractive error at age 15 years in ALSPAC participants (Fig 2A and 2B). The most strongly associated variant was rs188663068 (risk allele frequency (RAF) = 0.01, n = 3,819, p = 5.0×10^{-4}), each copy of the risk allele being associated with a -0.6 D shift in refractive error. Because SNPs in LD do not offer independent evidence of association, permutation testing was used to evaluate whether these results were likely to have arisen by chance. Consistent with the QQ-plot for the full set of SNPs tested (Fig 2B) permutation-based analysis suggested that obtaining a p-value as low as p = 5.0×10^{-4} for rs188663068 was not unexpected; however, such an excess of low p-values was unlikely to have occurred by chance (p = 1.4×10^{-2}). These findings are consistent with the notion that an excess of genetic variants in the promoter region and 5'-end of *APLP2* are associated with refractive error, but because the associated variants have a low minor allele frequency, no single SNP provides compelling evidence on its own. SNPs within 100 kb of the *APLP2* gene were also evaluated in a

meta-analyzed refractive error genome-wide association study (GWAS) dataset from the international Consortium for Refractive Error and Myopia (CREAM), which included 45,756 adult individuals from 27 Caucasian and 5 Asian cohorts [30]. As in the ALSPAC cohort, SNPs in the LD block encompassing the promoter region and 5'-end of the *APLP2* gene were most strongly associated with refractive error in the CREAM consortium sample (Fig 2C and 2D; top SNP, rs7127037, $p = 6.6 \times 10^{-3}$). The use of permutation testing to account for multiple testing was not possible for the CREAM dataset since we did not have access to the raw genotypes of individual participants. Therefore, as an alternative approach to test for an excess of low p-values in the region found to be associated in the ALSPAC cohort (hg19 chr 11:129904497– 129971498), the distribution of p-values inside this region was compared to the surrounding region encompassing 100 kb on the either side of the gene. P-values inside the region were skewed towards low values compared with the p-values outside the region ($p = 5.0 \times 10^{-3}$, two-sample Kolmogorov-Smirnov test, S1 Fig).

Gene-environment interaction between *APLP2* and time spent reading in children with myopia

To explore the possibility of an interaction between *APLP2* gene variants and visual experience, we exploited the availability of longitudinal refractive error measurements over childhood (age range 8 to 15 years) and prospective exposure information regarding the two most important currently known environmental risk factors for myopia, i.e., time spent reading and time spent outdoors. For the strongest *APLP2* risk variant, rs188663068, a "growth trajectory" analysis of refractive development revealed a progressive, age-dependent shift towards a relatively more myopic refractive error in individuals carrying a single copy of the high-risk "A" allele compared to individuals homozygous for the low-risk "G" allele ($p = 7.0 \times 10^{-3}$; Fig 3A and S2 Table). When analysed separately, time spent reading ascertained at age 8–9 years, and categorized as "high" or "low", was also predictive of refractive trajectory in ALSPAC participants, with the "high" reading group also gradually diverging towards a relatively more myopic refractive error as they became older ($p = 8.3 \times 10^{-9}$; Fig 3B and S3 Table). A model, which included both rs188663068 and time spent reading as predictors, provided strong evidence for a 3-way interaction between age, time spent reading at age 8–9 years and SNP genotype; implicating gene-environment interaction between the *APLP2* genetic variant and time spent reading that became greater with age (3-way interaction term, $p = 4.0 \times 10^{-3}$; S4 Table). Stratifying by time spent reading ("low" versus "high") revealed that the high-risk "A" allele of rs188663068 was predictive of progression towards myopia only in children who spent a "high" amount of time reading (genotype x age interaction term, $p = 0.99$ and $p = 7.1 \times 10^{-4}$ in "low" and "high" readers respectively; Fig 3C and 3D, S5 and S6 Tables). Logistic regression analysis in the ALSPAC participants at age 15 years confirmed the clinical relevance of the association at the *APLP2* locus (S7 and S8 Tables). The odds ratio (OR) for myopia associated with a single copy of the rs188663068 risk allele was 1.98 (95% CI = 1.02 to 3.87, $p = 4.5 \times 10^{-2}$), while by comparison the OR associated with a "high" amount of time spent reading at age 8 years was 1.61 (95% CI = 1.33 to 1.93, $p = 6.4 \times 10^{-7}$). Inclusion of an interaction term between rs188663068 genotype and time spent reading supported the presence of an interaction; the OR for myopia of participants in the "high" reading group and carrying a copy of the risk allele was 5.42 (95% CI = 1.15 to 25.52, $p = 3.3 \times 10^{-2}$). In linear regression analysis, time spent reading, alone, predicted 0.6% of the variance in refractive error at age 15 years, while the percentage of explained variance increased to 0.9% with the inclusion of rs188663068 genotype and a SNP/reading interaction term (S9 and S10 Tables). There was no evidence for an interaction between rs188663068 genotype and time spent outdoors (S11 and S12 Tables).
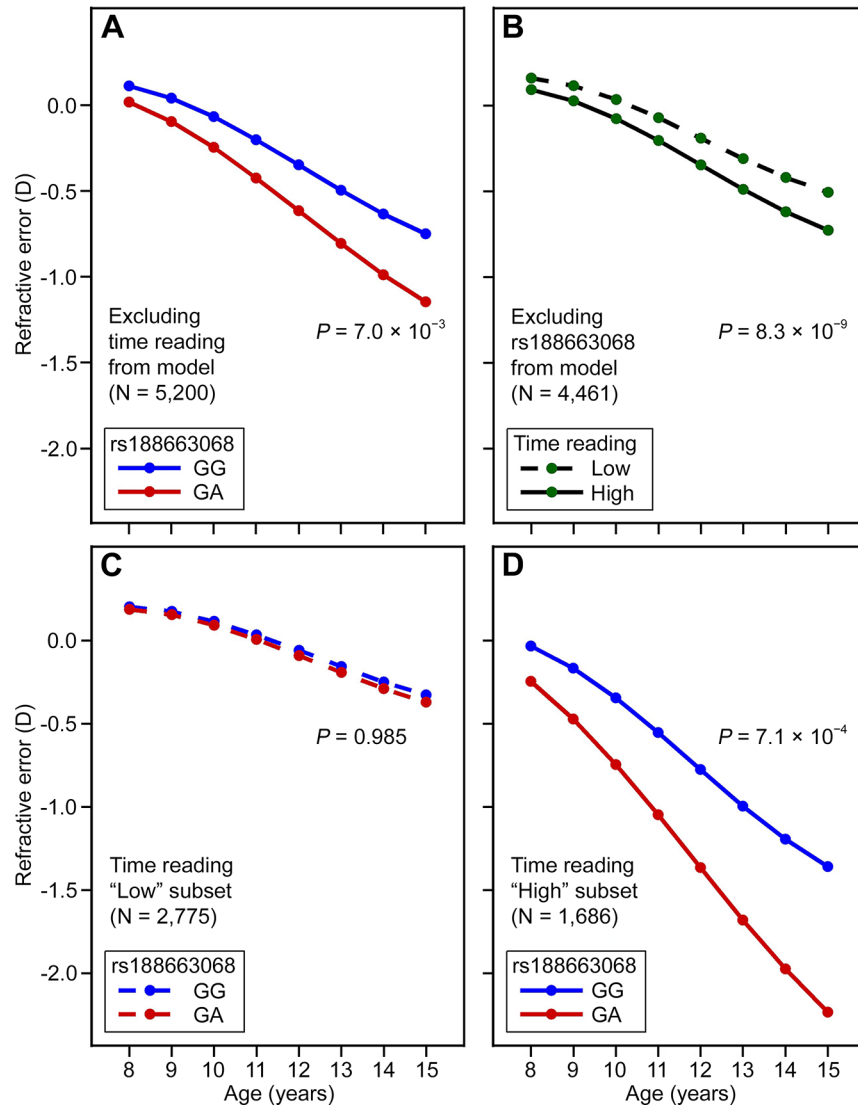
Fig 3. *APLP2* genotype and reading behaviour interact to influence refractive eye development in children. Refractive development in ALSPAC participants (n = 5,200) was modelled over the 8–15 year age range. Models included as a predictor variable either rs188663068 genotype (**A, C, D**) or a binary term categorizing children as spending a "high" or "low" amount of time reading at age 8½ years (**B**). Analyses used the full sample (**A**), those with information available on time spent reading (**B**), or a stratified sample consisting of the low (**C**) or high (**D**) readers.

doi:10.1371/journal.pgen.1005432.g003

Aplp2 regulates refractive eye development and susceptibility to myopia in mice

To examine whether *APLP2* is functionally involved in refractive error development, we studied refractive eye development in *Aplp2* knockout mice (Fig 4). Mice homozygous for a null allele of the *Aplp2* gene (*Aplp2$^{-/-}$* mice) were found to develop high degrees of hyperopia (+11.5 ± 2.2 D, p < 1.0×10^{-4}) compared to both heterozygous (*Aplp2$^{+/-}$*) (-0.8 ± 2.0 D, p < 1.0×10^{-4}) and wild-type (*Aplp2$^{+/+}$*) (+0.3 ± 2.2 D, p < 1.0×10^{-4}) littermates (Fig 4A), consistent with the finding that *APLP2* expression is suppressed in hyperopia in monkeys (Fig 1). Visual form deprivation induced -1.2 ± 0.6 D of myopia (p = 3.0×10^{-2}) in *Aplp2$^{-/-}$*
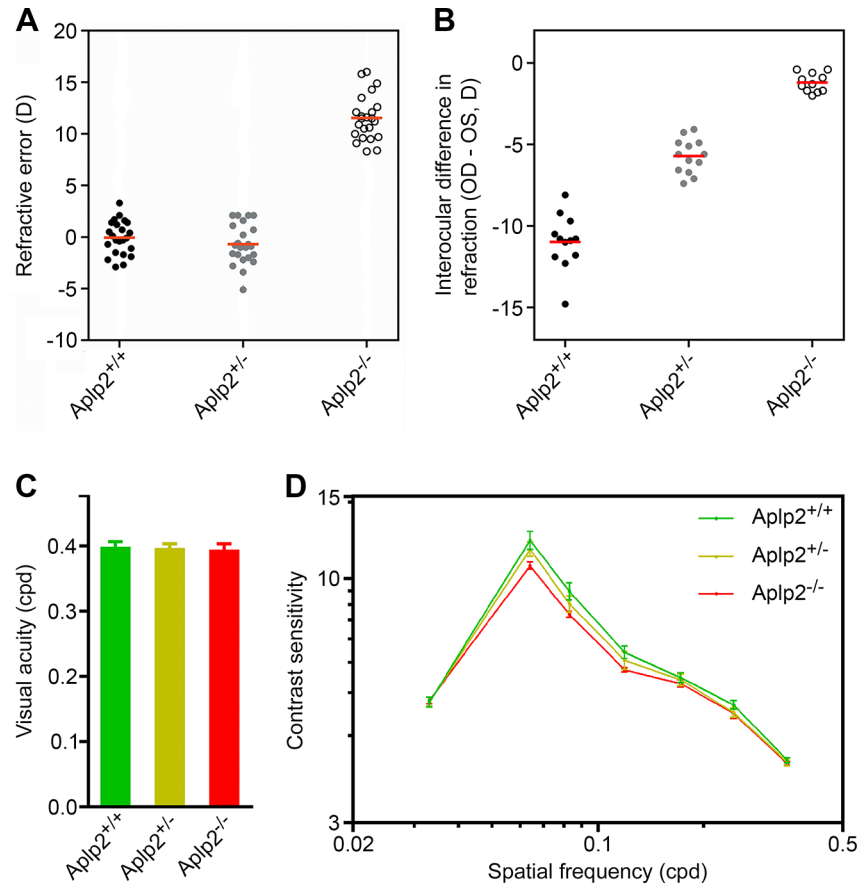
Fig 4. *Aplp2* regulates refractive eye development in the mouse. (**A**) Effect of targeted deletion of *Aplp2* on refractive eye development in the mouse. *Aplp2* knockout mice (generated on C57BL/6J background) develop high degrees of hyperopia (+11.5 ± 2.2 D, $p < 1.0 \times 10^{-4}$) compared to both heterozygous (-0.8 ± 2.0 D, $p < 1.0 \times 10^{-4}$) and wild-type (+0.3 ± 2.2 D, $p < 1.0 \times 10^{-4}$) littermates. Refractive errors were measured at P35 (age when refractive errors stabilize in mice) using automated infrared photorefractor. Red horizontal bars, mean. (**B**) Effect of targeted deletion of *Aplp2* on susceptibility to experimental myopia in mice. Lack of *Aplp2* expression had a negative dose-dependent effect on susceptibility to myopia in mice. Visual form deprivation (VFD) induced -1.2 ± 0.6 D of myopia ($p = 3.0 \times 10^{-2}$) in the *Aplp2* knockouts compared to -5.7 ± 1.1 D ($p < 1.0 \times 10^{-4}$) in heterozygous and -11.0 ± 1.7 D ($p < 1.0 \times 10^{-4}$) in wild-type littermates. VFD was carried out for 21 days from P24 through P45 and refractive status of the deprived eyes versus control eyes was measured using an automated infrared photorefractor (Methods). Red horizontal bars, mean. (**C**) Effect of targeted deletion of *Aplp2* on visual acuity in mice. Visual acuity in *Aplp2* knockouts was not significantly different from that in the heterozygous and wild-type littermates ($F_{(2, 20)} = 0.6$, $p = 0.58$). Error bars, s.d.; n = 13. (**D**) Effect of targeted deletion of *Aplp2* on contrast sensitivity in mice. Lack of *Aplp2* resulted in a dose-dependent reduction in contrast sensitivity ($F_{(12, 120)} = 3.6$, $p = 1.5 \times 10^{-4}$). Error bars, s.d.; n = 13. Both visual acuity and contrast sensitivity were measured at P80 using a mouse virtual optomotor system.

doi:10.1371/journal.pgen.1005432.g004

mice compared to -5.7 ± 1.1 D ($p < 1.0 \times 10^{-4}$) in *Aplp2*$^{+/-}$ heterozygotes and -11.0 ± 1.7 D ($p < 1.0 \times 10^{-4}$) in wild-type littermates, indicating that lack of *Aplp2* expression has a dose-dependent inhibitory effect on susceptibility to environmentally induced myopia ($F_{(2, 33)} = 191.0$, $p < 1.0 \times 10^{-4}$) (Fig 4B), thus confirming gene-environment interaction between *APLP2* and visual experience identified by human studies.

Aplp2 regulates refractive eye development by modulating the function of glycinergic amacrine cells of the retina

Visual acuity in *Aplp2$^{-/-}$* mice was not different from that in heterozygous and wild-type litter-mates ($F(2, 20) = 0.6$, $p = 0.58$) ([Fig 4C](#) and [S13 Table](#)), whereas contrast sensitivity was reduced compared to both heterozygous and wild-type mice ($F(12, 120) = 3.6$, $p = 1.5 \times 10^{-4}$) ([Fig 4D](#) and [S13 Table](#)). Analysis of scotopic ERGs in *Aplp2* knockouts revealed that lack of *Aplp2* caused a dose-dependent decrease in the amplitude of the b-wave ($F(2, 18) = 6.9$, $p = 6.0 \times 10^{-3}$) ([Fig 5A and 5B and 5D](#)) and oscillatory potentials ($F(2, 18) = 3.6–20.5$, $p < 1.0 \times 10^{-3}$) ([Fig 5F and 5G](#)); as well as an increase in the implicit time of the b-wave ($F(2, 18) = 6.1$, $p = 9.6 \times 10^{-3}$) ([Fig 5C and 5E](#)) and oscillatory potentials ($F(2, 18) = 4.5–20.9$, $p < 5.0 \times 10^{-3}$) ([Fig 5F and 5H](#)). Considering that oscillatory potentials are primarily generated by retinal amacrine cells [56,57], which also modulate the amplitude of the b-wave generated by the bipolar cells [58–66], the ERG data suggested that *Aplp2* modulates the function of amacrine cells. Therefore, we then analyzed the expression of *Aplp2* in the retina at the mRNA and protein levels. *In situ* hybridization and immunohistochemical analysis confirmed *Aplp2* expression in both bipolar and amacrine cells of wild-type mice ([Fig 6A–6C](#) and [S2 Fig](#)). Further analysis also revealed that *Aplp2* was expressed in glycinergic amacrine cells, but was not expressed in GABAergic amacrines (Figs [6D and 6E](#) and [S2](#)).

Discussion

More than 24 chromosomal loci associated with human myopia have been identified [15,25,26,29–31,67–89] either by linkage analysis, which primarily focuses on rare variants with large effect size causing Mendelian forms of myopia, or by large-scale GWAS studies, targeting common variants with moderate effect sizes underlying common myopia. However, refractive error is inherited as a complex quantitative trait thought to be influenced by multiple interacting genes and controlled by dozens and even hundreds of chromosomal loci [19,90–92]. The variants identified to date account for less than 10% of common myopia cases [31], suggesting the existence of a large number of yet unidentified low-frequency and/or small-effect variants, which underlie the majority of myopia cases [32–35].

Several approaches for finding the "missing heritability" of complex traits have been proposed (e.g., increasing GWAS sample sizes, using larger catalogues of human variation, including copy number variations in analyses etc.); however, the most promising route for identification of missing low-frequency and small-effect variants lies through combining biological functional evidence with statistical genetic evidence [33].

Here, we used such "systems genetics" approach, combining gene expression profiling in an animal model of myopia, statistical evidence for association with myopia from two GWAS studies, and functional evidence from a gene-targeted mouse model, to identify *APLP2* as one of the "missing" myopia genes. *APLP2* was first found to be differentially expressed in the retina of monkeys with experimentally-induced myopia. We then found that numerous SNPs within the 5'-end of *APLP2* were associated with refractive error development in children and adults. Furthermore, *Aplp2* also strongly influenced refractive eye development and myopia susceptibility in the gene-targeted mouse model of myopia. Interestingly, *APLP2* is also localized within a broad suggestive myopia locus with LOD score 3.2 identified by Hammond et al. on chromosome 11q23-24 [93].

APLP2 was first identified as a homologue of the amyloid beta (A4) precursor protein (*APP*) [50] and was assigned to the human chromosome 11q23-25 [49] and the proximal region of mouse chromosome 9 [47]. It was also found that the expression pattern of *APLP2* resembles that of *APP* in the brain and throughout the body, with particularly high expression
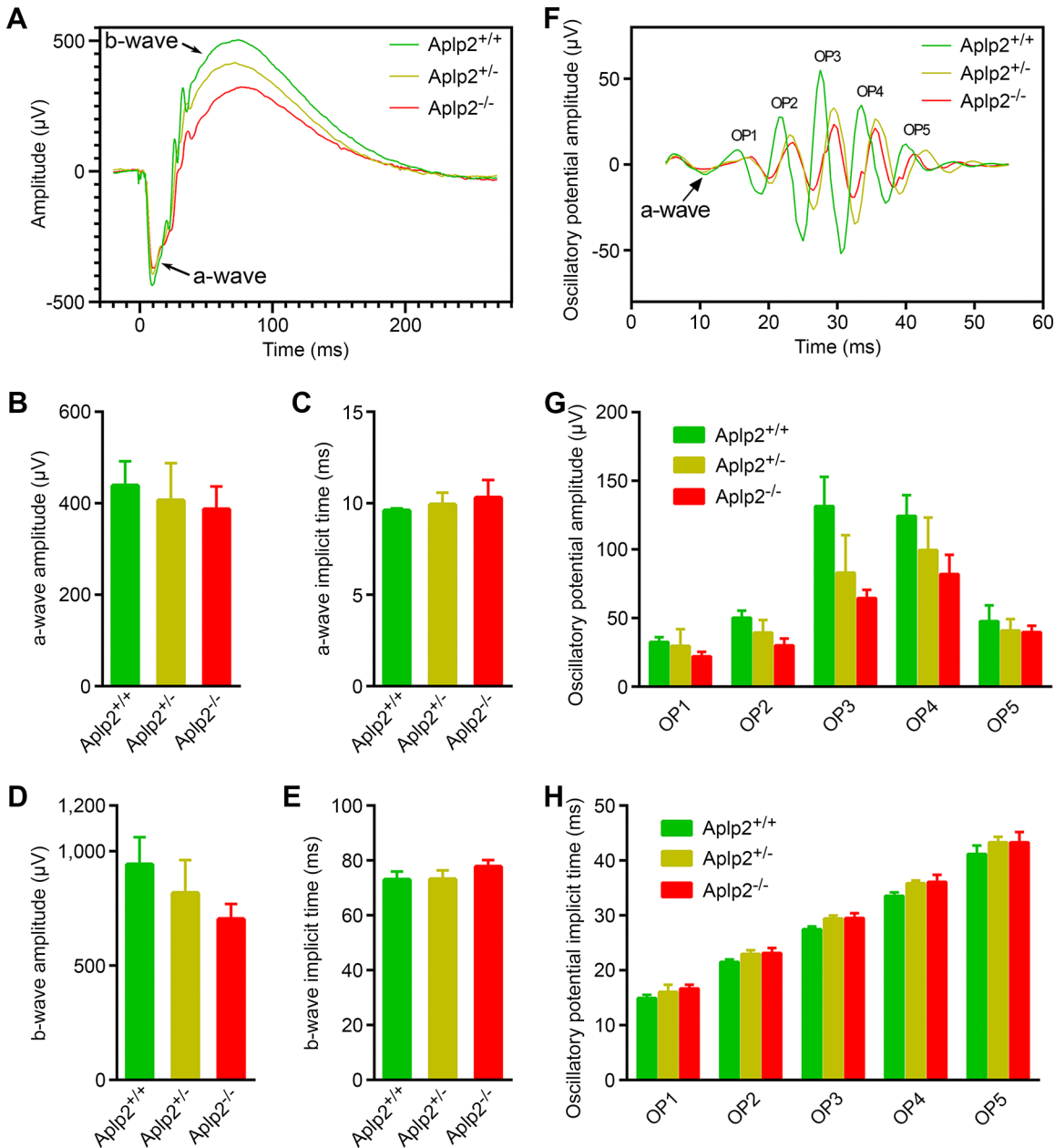
Fig 5. Analysis of scotopic electroretinograms in the *Aplp2* knockout mice. (A-E) Effect of targeted deletion of *Aplp2* on the a-wave and b-wave. Lack of *Aplp2* causes a dose-dependent decrease in the b-wave amplitude ($F_{(2, 18)} = 6.9$, $p = 6.0 \times 10^{-3}$). The b-wave implicit time was increased in the *Aplp2* knockouts compared to both heterozygous and wild-type littermates ($F_{(2, 18)} = 6.1$, $p = 9.6 \times 10^{-3}$). Lack of *Aplp2* did not have significant impact on either a-wave amplitude or a-wave implicit time ($F_{(2, 18)} = 0.8$, $p = 0.47$, amplitude; $F_{(2, 18)} = 2.6$, $p = 0.1$, implicit time). **(F-H)** Effect of targeted deletion of *Aplp2* on oscillatory potentials. The amplitude of the oscillatory potentials (OP) exhibited a dose-dependent decrease in the *Aplp2* knockout mice, while the OP implicit time was increased in both heterozygous and knockout animals compared to the wild-type littermates. OP1 amplitude: $F_{(2, 18)} = 3.6$, $p = 5.0 \times 10^{-2}$; OP2 amplitude: $F_{(2, 18)} = 15.6$, $p = 1.0 \times 10^{-4}$; OP3 amplitude: $F_{(2, 18)} = 20.5$, $p < 1.0 \times 10^{-4}$; OP4 amplitude: $F_{(2, 18)} = 9.7$, $p = 1.0 \times 10^{-3}$; OP5 amplitude: $F_{(2, 18)} = 1.9$, $p = 0.2$; OP1 implicit time: $F_{(2, 18)} = 7.2$, $p = 5.0 \times 10^{-3}$; OP2 implicit time: $F_{(2, 18)} = 10.9$, $p = 8.0 \times 10^{-4}$; OP3 implicit time: $F_{(2, 18)} = 20.9$, $p < 1.0 \times 10^{-4}$; OP4 implicit time: $F_{(2, 18)} = 17.7$, $p < 1.0 \times 10^{-4}$; OP5 implicit time: $F_{(2, 18)} = 4.5$, $p = 3.0 \times 10^{-2}$. Error bars, s.d.; n = 7.

in neurons of the central and peripheral nervous system [50,94]. The biological role of *APLP2* was investigated using gene-targeted mouse mutants. *Aplp2* knockout mice were normal in size, fertile, and appeared healthy, whereas 80% of *Aplp2/APP* double knockout animals died
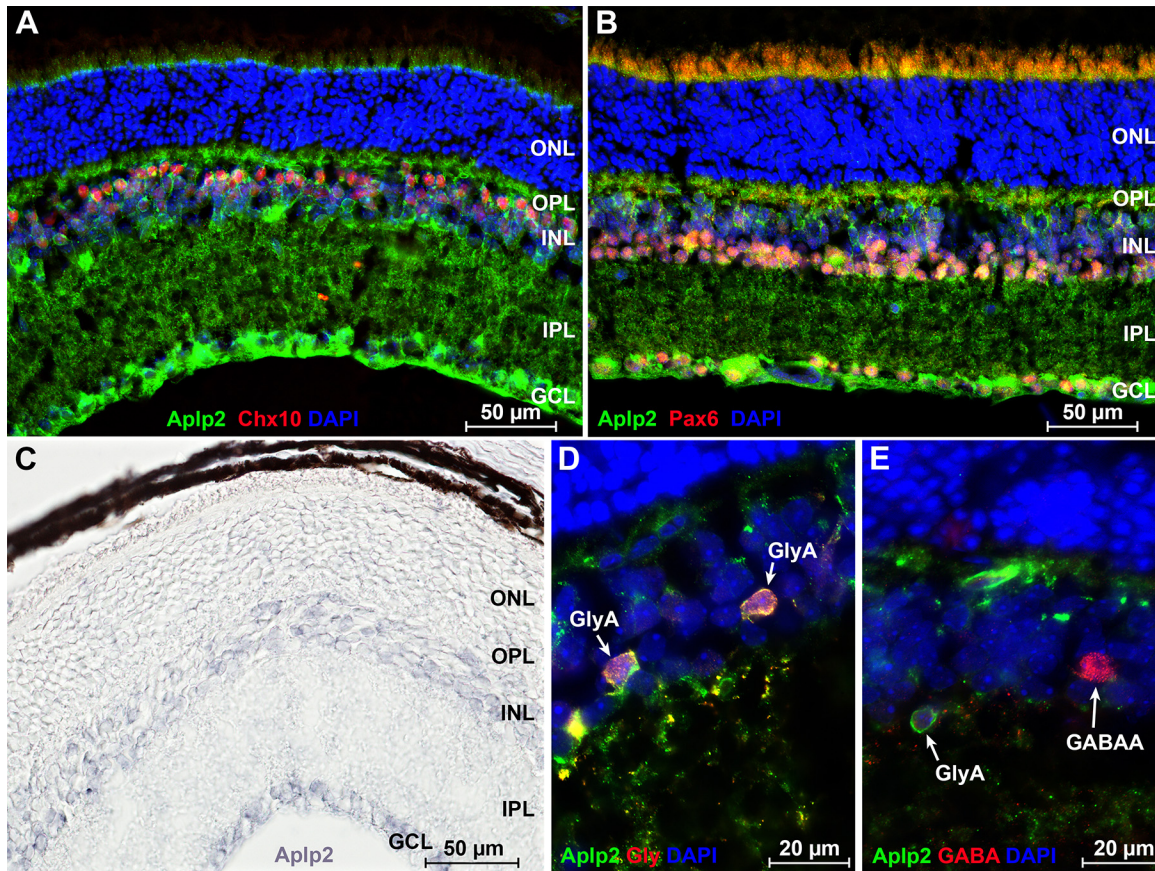
Fig 6. Analysis of *Aplp2* expression in the retina. (**A**) Double staining with antibodies to Chx10 (red), which label bipolar cells, and Aplp2 (green) demonstrate that *Aplp2* is expressed in the bipolar cells of the retina. (**B**) Double staining with antibodies to Pax6 (red), which label amacrine cells, and Aplp2 (green) demonstrate that Aplp2 is expressed in the amacrine cells of the retina. Expression of *Aplp2* is also observed in the ganglion cell layer. (**C**) Analysis of *Aplp2* expression in the retina at the mRNA level using *in situ* hybridization. *In situ* revealed that *Aplp2* is expressed in the inner nuclear and ganglion cell layers of the retina. (**D**) Double staining with antibodies to glycine (red) and Aplp2 (green) revealed that *Aplp2* is strongly expressed in the glycinergic amacrines. Arrows show two glycinergic amacrines with high levels of *Aplp2* expression. (**E**) Double staining with antibodies to GABA (red) and Aplp2 (green) demonstrated that *Aplp2* is not expressed in the GABAergic amacrines. Arrows show a glycinergic amacrine with strong expression of *Aplp2* and an Aplp2-negative GABAergic amacrine. Blue, cell nuclei counterstained with DAPI. GABA, gamma-Aminobutyric acid; GABAA, GABAergic amacrine; GCL, ganglion cell layer; Gly, glycine; GlyA, glycinergic amacrine; INL, inner nuclear layer; IPL, inner plexiform layer; ONL, outer nuclear layer; OPL, outer plexiform layer.

doi:10.1371/journal.pgen.1005432.g006

within 24 h after birth and the remaining 20% exhibited difficulty in righting, ataxia, spinning behavior, and a head tilt [45,52,95]. This was contrasted by no lethality or apparent abnormalities in *Aplp1/APP* double knockouts, suggesting that the *Aplp2* plays a key role in neuronal development and function [52,95–97]. In the brain, APLP2 protein has been localized to the presynaptic active zone of neuronal axons in close proximity to the synaptic vesicles [36]. Consistent with these data, it has been reported that the lack of an Aplp2/APP complex results in reduced expression of vesicular glutamate transporter 2 (*VGLUT2*) and a defect in synaptic transmission [40,41], as well as reduced spatial learning and synaptic plasticity [37–39]. These effects of *Aplp2* on neuronal function have been suggested to be mediated by its role in the subtle modulation of neurotransmitter release [36,39]. Our observation in mice that *APLP2* modulates the electrophysiological properties of the retina is consistent with its role in synaptic transmission. We found that lack of *Aplp2* led to a significant dose-dependent suppression of the b-wave and oscillatory potentials of the ERG. Considering that oscillatory potentials are primarily generated by the amacrine cells [56,57], which also modulate the amplitude of the

b-wave generated by the bipolar cells [58–66], the ERG data suggest that *Aplp2* influences refractive eye development by modulating the function of amacrine cells. Interestingly, this is consistent with a previously suggested role for amacrine cells in the regulation of refractive eye development [98–108]. The involvement of *Aplp2* in the regulation of retinal processing at the level of amacrine cells is further corroborated by our findings that *Aplp2* is expressed in the glycinergic amacrine cells of the retina, which provide feed-forward and feedback inhibition in the retina and play important role in contrast processing [109–115].

Retinal blur associated with inaccurate accommodation during nearwork (so called accommodative lag) and peripheral hyperopic defocus have been hypothesized to be the driving force behind myopia progression in children [116–118]. We found that *Aplp2* modulated sensitivity to retinal image degradation induced by form-deprivation in a dose-dependent manner, yet, lack of *Aplp2* did not cause an observable change in visual acuity. Thus, our data, in conjunction with the published data on the role of *APLP2* in neuronal function, suggest that *APLP2* most likely modulates sensitivity to the degradation of retinal images by regulating the processing of contrast by the retina via modulation of synaptic transmission at the level of glycinergic amacrines. The reduced susceptibility to myopia in mice lacking *Aplp2* makes lowering the level of APLP2 in the retina via gene therapy an appealing future direction for therapeutic intervention in human myopia.

In summary, we have identified *APLP2* as a novel gene involved in refractive eye development and associated with human myopia. The role of *APLP2* in human myopia is supported by several lines of evidence, which suggest that genetic variation at the *APLP2* promoter region may influence *APLP2* expression in the inner retina and, in turn, may modulate synaptic transmission at the level of amacrine cells, leading to alterations in refractive development. Consistent with its important role in neuronal development and function, *APLP2* appears to have been subject to intense evolutionary pressure evidenced by 97.7% DNA sequence conservation of the gene between humans and mice. Our findings that naturally occurring genetic variation at the *APLP2* locus was associated with myopia only in children who spent an above-average time reading and observations of an analogous gene-environment interaction between *Aplp2* and visual input in mice also imply a high level of evolutionary conservation for the pathways underlying refractive eye development. Further work will be required to pinpoint the causal variant(s) at the *APLP2* locus that determine susceptibility to myopia, and to elucidate whether (as suggested by the location of the most strongly associated variant in the promoter region of the gene) they alter the level of *APLP2* expression. Future functional studies will also need to explore the role of *APLP2* in synaptic transmission at the level of amacrine cells and its role in defocus processing.

Materials and Methods

Tests for association with genetic variants at the *APLP2* locus in children

To investigate whether naturally-occurring genetic variation at the *APLP2* locus influences refractive development in children, data from an existing British birth cohort were examined. The Avon Longitudinal Study of Parents and Children (ALSPAC) recruited 14,541 pregnant women resident in Avon, UK with expected dates of delivery 1st April 1991 to 31st December 1992. Of the initial 14,541 pregnancies, 13,988 children were alive at 1 year. Data collected included self-completion questionnaires sent to the mother, to her partner and after age 5 to the child; direct assessments and interviews in a research clinic; biological samples and linkage to school and hospital records. The original cohort was largely representative of the UK 1991 Census; however, there was trend for greater loss at follow-up for families of low socio-economic status and of non-White ethnic origin [119]. Ethical approval for the study was

obtained from the ALSPAC Law and Ethics committee and the three local research-ethics committees.

Refractive error was assessed using non-cycloplegic autorefraction at research clinics attended when children were approximately 7½, 10½, 11½, 12½ and 15½ years of age [120]. DNA samples from the participants were genotyped on Illumina HumanHap 550 bead arrays [121]. Data were available for a total of 464,311 autosomal SNPs that passed quality control filters [121] in 8,365 individuals of European ancestry (as demonstrated by clustering with Hap-Map CEU individuals upon multidimensional scaling analysis). SNPs at non-genotyped loci were imputed with MACH,[122] using the 1000-genomes project GIANT consortium November 2010 data release as a reference panel. For attendees at the 15½ year clinic (n = 3,819), association between non-cycloplegic refractive error and imputed genotype dosage was tested using mach2qtl for SNPs within 100 kb of the *APLP2* gene. Age and sex were included as covariates in the analysis. Permutation testing was used to generate empirical p-values that accounted for multiple testing and for LD between markers. It was carried out by assigning subjects a new phenotype, sampled randomly without replacement from the true list of phenotypes, and repeating the tests for association between the new trait and the genotype for all SNPs in the region. From 1000 such permutations, the probability of observing a p-value as low as that found in the real dataset was estimated. To test for an excess of low p-values, the probability of observing the 5th percentile p-value from the real dataset was estimated from the 5th percentile p-values observed in the 1000 permutations.

To explore whether the most strongly associated SNP at the *APLP2* locus, rs188663068, acted early or late in childhood, the imputed genotype for this SNP was included as a fixed effect term in a linear mixed model of childhood refractive error "trajectory" in ALSPAC participants (note that because of the very low risk allele frequency (RAF) of rs188663068, the single subject who was homozygous for the risk allele (genotype AA) was re-coded as a heterozygote (GA). The model also included sex, age, age^2 and age^3 as fixed effects, while refractive error over the age range 7½ to 15½ years and a linear age term were modelled as random effects. Data were included for 5,200 ALSPAC participants for whom non-cycloplegic autorefraction readings had been obtained on at least 3 occasions (specifically, there were 833 subjects with data available from 3 visits, 1,696 with data from 4 visits, and 2,671 with data from all 5 visits). Linear mixed modelling was performed using the *lme* function in R.

More complex refraction trajectory models were constructed by including additional predictor variables. Time spent reading was ascertained from a questionnaire completed by the mother when the ALSPAC participants were aged approximately 8½ years as previously described [120]. In response to the question "On normal days in school holidays, how much time on average does your child spend each day reading books for pleasure", children were classified as either spending a "high" (response "1–2 hours" or "3 or more hours" per day) or "low" (response "None at all" or "1 hour or less") amount of time reading. The time reading variable was coded as "low" = 0 (reference) and "high" = 1. There were 2,775 and 1,686 subjects in the "low" and "high" subsets, respectively (note that information on time spent reading was missing for 739 of the 5,200 participants in the refraction trajectory sample). Although time spent reading was sampled at only a single age-point, reading behaviour may track forward as children get older. Therefore, the time spent reading variable's predictive capacity may stem from capturing inter-subject variation not only at the age of 8–9 years, but also to some extent inter-subject variation in reading behaviour at older ages. Time spent outdoors was gauged from a separate item on the same questionnaire: "On a school weekday, how much time on average does your child spend each day out of doors in summer?". Children were classified as spending a "high" amount of time outdoors if the response was "1–2 hours" or "3 or more hours", and as "low" otherwise. Note that this questionnaire response was selected for the

present study instead of a closely-related one used previously [120], since the former provided an approximately equal split of the sample, while the latter variable resulted in an ~1:9 ratio of subjects classified as spending a low versus high amount of time outdoors, and thus despite its slightly greater predictive discrimination of incident myopia, it would have led to very small numbers of subjects in the "low time outdoors + GA rs188663068 genotype" group. The time outdoors variable was coded as "low" = 0 (reference, n = 2,349) and "high" = 1 (n = 2,145) and there were 706 children with missing information. Sex was not significantly associated with refractive error in the refraction trajectory analyses and so was dropped from the models.

To confirm the refraction trajectory results, association between rs188663068 genotype (coded GG = 0, GA = 1) and refractive error was also analyzed using linear and logistic regression for subjects attending the ALSPAC research clinic; targeting the children when aged 15 years. All children with information available were included in these models to maximise precision of risk estimates. Time spent reading and time spent outdoors were included, separately, as predictors, using the coding scheme described above, in models with and without an interaction term (rs188663068 genotype x time reading, etc.). Sex was not significantly associated with refractive error in these linear regression analyses and so was dropped from the models. Age-at-baseline was not included since, being a birth cohort, the age interval was narrow at each target age. As in the refraction trajectory analyses, the single subject with rs188663068 genotype AA was re-coded as GA.

Tests for association with genetic variants at the *APLP2* locus in adults

Genetic variants at the *APLP2* locus were examined using meta-analyzed data from the international genome-wide association study (GWAS) of refractive error carried out by the Consortium for Refractive Error and Myopia (CREAM) [30]. The CREAM meta-analysis included data from 32 studies: 1958 British Birth Cohort, ALSPAC (mothers), ANZRAG, AREDS1a1b, AREDS1c, Beijing Eye Study, BMES, CROATIA-Korcula, CROATIA-Split, CROATIA-Vis, DCCT, EGCUT, ERF, FECD, FITSA, Framingham, GHS 1, GHS 2, KORA, OGP Talana, ORCADES, RS1, RS2, RS3, SCES, SIMES, SINDI, SP2, TEST/BATS, TwinsUK, WESDR, and YFS. Each study received prior approval from its local medical ethics committee, and written informed consent was obtained from all participants in accordance with the tenets of the Declaration of Helsinki. The age of subjects in each sample ranged from 31.4 to 79.9 years and, apart from 3 samples, contained an approximately equal split of males/females. Twenty-seven samples comprised of subjects of European ancestry, while 5 were of Asian ancestry. GWAS analyses were carried out for spherical equivalent refractive error (dependent variable) with genotype dosage, age and sex included as independent variables, and meta-analysis was done under a random-effects model, as described [30]. SNPs within 100 kb of the *APLP2* gene were evaluated. Permutation-based analysis to correct for multiple testing could not be carried out for the CREAM GWAS dataset since we did not have access to the raw genotypes. Therefore, for SNPs within 100 kb of *APLP2*, the distribution of CREAM p-values inside versus outside the region showing strong association in the ALSPAC sample (hg19 chr 11:129904497–129971498; hg18 chr 11:129409707–129476708) was compared using the two-sample Kolmogorov-Smirnov test.

Aplp2 knockout mice

Aplp2 knockout mice (B6.129S7-Aplp2^{tm1Dbo}/J) were obtained from the Jackson Laboratory (Bar Harbor, ME) as heterozygotes and were maintained as an in-house breeding colony on a C57BL/6J background, which was shown not to carry Rd mutations that cause retinal degeneration in mice [123]. To generate homozygous (*Aplp2$^{-/-}$*), heterozygous (*Aplp2$^{+/-}$*) and wild-type

($Aplp2^{+/+}$) animals for the experiments, heterozygous males and females were bred and resulting offspring were genotyped as previously described [45] to identify animals of different genotypes. Only littermates were used for all experiments to ensure isogenic genetic background. All animals received water and food ad libitum. All mouse procedures adhered to the ARVO Statement for the Use of Animals in Ophthalmic and Vision Research and were approved by the Columbia University Institutional Animal Care and Use Committee (Protocol #AAAK2700). Animals were anesthetized via intraperitoneal injection of pentobarbital (50 mg/kg), or via intraperitoneal injection of ketamine (90 mg/kg) and xylazine (10 mg/kg). Animals were euthanized by cervical dislocation while under full surgical anesthesia.

Analysis of refractive eye development in *Aplp2* knockout mice

Visually guided emmetropization normally results in children who are born myopic becoming less myopic and children who are born hyperopic becoming less hyperopic during the early postnatal period [1]. In mice, both the variability and magnitude of the refractive error are reduced during the early postnatal period (P21-P40) indicating emmetropization [124–126]. In C57BL/6J mice, refractive error stabilizes around emmetropia at ~P32. To examine the role of *Aplp2* in emmetropization, we analyzed refractive eye development in mice homozygous ($Aplp2^{-/-}$) and heterozygous ($Aplp2^{+/-}$) for a null allele of the *Aplp2* gene, as well as in the wild-type animals ($Aplp2^{+/+}$). The refractive state of both left and right eyes was determined on alert animals at P21, P35, and P67 using an automated eccentric infrared photorefractor as previously described [124,127]. The animal to be refracted was immobilized using a restraining platform, and each eye was refracted along the optical axis in dim room light (< 1 lux), 20–30 min. after instilling 1% tropicamide ophthalmic solution (Alcon Laboratories, Inc., Fort Worth, TX) to ensure mydriasis and cycloplegia. Five independent measurement series (~300–600 measurements each) were taken for each eye. The measurements were automatically acquired by the photorefractor every 16 msec. Each successful measurement series (i.e., Purkinje image in the center of the pupil and stable refractive error for at least 5 sec.) was marked by a green LED flash, which was registered by the photorefractor software. Sixty individual measurements from each series, immediately preceding the green LED flash, were combined, and a total of 300 measurements (60 measurements x 5 series = 300 measurements) were used to calculate the refractive error mean and standard deviation.

Analysis of gene-environment interaction between *Aplp2* and visual experience in *Aplp2* knockout mice

Human population studies revealed that environmental factors, such as nearwork and reading, play important role in the development of myopia [128–131]. These findings were complemented by observations that nearwork and reading are associated with the lag of accommodation, i.e., insufficiently strong accommodative response for near objects, which places the plane of best focus behind the retina (producing slight optical blur) when the subject performs nearwork tasks [116,117]. Optical blur produced by the lag of accommodation is the signal that drives excessive eye growth and causes myopia [116,129,132–135]. Animal studies also demonstrated that excessive eye growth and myopia can be induced in species as diverse as the fish, chicken, tree shrew, monkeys, guinea pig and, most recently, mouse by retinal image degradation or optical blur (recapitulated in animal models by placing a diffuser or a negative lens in front of the eye) [136–143].

To examine the role of *Aplp2* in the development of environmentally induced myopia, we analyzed the effect of diffuser-imposed retinal image degradation (visual form deprivation) on refractive eye development in mice homozygous ($Aplp2^{-/-}$) and heterozygous ($Aplp2^{+/-}$) for a

null allele of the *Aplp2* gene, as well as in the wild-type mice (*Aplp2*$^{+/+}$). Visual input was degraded in one of the eyes by applying plastic diffusers, and refractive development of the treated eye was compared to that of the contralateral eye, which was not treated with a diffuser, as previously described [126,143]. Diffusers represented low-pass optical filters, which severely degraded the image projected onto the retina by removing high spatial frequency details. Frosted hemispherical plastic diffusers were hand-made using caps from 0.2 ml PCR tubes (Molecular BioProducts, San Diego, CA) and rings made of medical tape (inner diameter 6 mm; outer diameter 8 mm). A cap was frosted with fine sandpaper and attached to a ring with Loctite Super Glue (Henkel Consumer Adhesives, Avon, OH). On the first day of the experiment (P24), animals were anesthetized via intraperitoneal injection of pentobarbital (50 mg/kg), and diffusers were attached to the skin surrounding the right eye with three stitches using size 5–0 ETHILON microsurgical sutures (Ethicon, Somerville, NJ) and reinforced with Vetbond glue (3M Animal Care Products, St. Paul, MN) (the left eye served as a control). Toenails were covered with adhesive tape to prevent mice from removing the diffusers. Animals recovered on a warming pad and were then housed under low-intensity constant light in transparent plastic cages for the duration of the experiment as previously described [126,143]. Following 21 days of visual form deprivation (from P24 through P45), diffusers were removed and refractive status of both treated and control eyes was assessed using an automated eccentric infrared photorefractor as previously described [144]. The interocular difference in refraction between the treated and contralateral control eye served as an indication of the extent of induced myopia.

Analysis of visual acuity and contrast sensitivity in *Aplp2* knockout mice

To examine the role of *Aplp2* in the overall visual function, we compared visual acuity and contrast-sensitivity in the *Aplp2* knockout mice (*Aplp2*$^{-/-}$), mice heterozygous (*Aplp2*$^{+/-}$) for a null allele of the *Aplp2* gene, and in the wild-type littermates (*Aplp2*$^{+/+}$). Both visual acuity and contrast sensitivity were measured at P80 using a virtual optomotor system (Mouse OptoMotry System, Cerebral Mechanics, Medicine Hat, AB Canada), as previously described [145]. Briefly, the animal to be tested was placed on a platform surrounded by four computer screens displaying a virtual cylinder comprising a vertical sine wave grating in 3D coordinate space. The OptoMotry software controlled the speed of rotation, direction of rotation, the frequency of the grating and its contrast.

To measure visual acuity, the initial spatial frequency of the grating was set at 0.1 cycles/degree and the contrast was set at maximum. The frequency was then systematically increased using staircase procedure until the maximum spatial frequency capable of eliciting a response (visual acuity) was determined. The staircase procedure was such that 3 correct answers in a row advanced it to a higher spatial frequency, while 1 wrong answer returned it to a lower frequency.

Contrast sensitivity function was measured at seven spatial frequencies, i.e. 0.033, 0.064, 0.083, 0.119, 0.172, 0.244, and 0.347 cycles/degree, using the staircase procedure described above. The contrast sensitivity at each frequency was calculated as a reciprocal of the contrast threshold, which was calculated as a Michelson contrast from the screen luminances ($\frac{I_{max} - I_{min}}{I_{max} + I_{min}}$; I_{white} = 208.25 cd/m^2, I_{black} = 0.21 cd/m^2).

Analysis of electrophysiological properties of the mouse retina

Dark-adapted electroretinograms (ERGs) are particularly sensitive to changes in the inner retina [56]; therefore, to assess the effect of *Aplp2* on the electrophysiological properties of various neuronal populations in the retina, we analyzed scotopic ERGs in the *Aplp2* knockout

($Aplp2^{-/-}$) mice, mice heterozygous for a null allele of the *Aplp2* gene ($Aplp2^{+/-}$ mice), and in the wild-type littermates ($Aplp2^{+/+}$ mice). Animals to be used for ERG were dark-adapted overnight. Prior to ERG recordings, dark-adapted mice were anesthetized via intraperitoneal injection of ketamine (90 mg/kg) and xylazine (10 mg/kg) and placed on a heating pad. The pad was connected to a rectal probe and thermostat via a feedback circuit, which maintained the body temperature at 37°C. Pupil dilation was achieved by instilling one drop of 1% tropicamide ophthalmic solution (Alcon Laboratories, Inc., Fort Worth, TX) in each eye at the time of anesthesia. Silver-embedded thread corneal recording electrodes were positioned across the apex of each cornea anesthetized with Lidocaine and held in place with 2.5% Goniovisc ophthalmic solution (HUB Pharmaceuticals, Rancho Cucamonga, CA) and optically clear mini contact lenses (Ocuscience, Rolla, MO). Stainless steel sub-dermal needle reference electrodes were placed subcutaneously below each eye along the upper jaw, while the ground electrode was inserted into the base of the tail. ERGs were recorded using Ocuscience rodent ERG system (Rolla, MO). To elicit retinal responses, each eye was presented with 5-msec white-light flashes of increasing intensity produced by a mini-Ganzfeld stimulator. Nine intensities ranging from 0.001 cd•s/m^2 to 32 cd•s/m^2 were used with the interstimulus interval increasing from 18 sec to 120 sec with the increase in the stimulus intensity (12-sec increase for each step). Responses to three flashes of each intensity were recorded and averaged. ERG data were processed and quantified using ERGVIEW software package (Ocuscience, Rolla, MO).

Analysis of *Aplp2* expression in the eye

To identify the tissues and cell types in which *Aplp2* is expressed, we examined expression of *Aplp2* in the eye using *in situ* hybridization and immunohistochemistry. *In situ* hybridizations were performed essentially as previously described [146]. Briefly, C57BL/6J mouse eyes were enucleated at P27 and used to prepare eyecups by removing the cornea and lens in ice-cold 1 X PBS. The eyecups were then fixed in 4% paraformaldehyde in 1 X PBS overnight at 4°C, cryoprotected in 30% sucrose in 1 X PBS and embedded in Tissue-Tek O.C.T compound (Sakura Finetek USA, Torrance, CA). 10-μm cryostat sections were incubated with 1 μg/ml Proteinase K in 1 X PBS, washed in 2 mg/ml Glycine in 1 X PBS, incubated with 0.25% acetic anhydride in 0.1 M TEA buffer, and hybridized with digoxigenin(DIG)-labeled cDNA probes followed by incubation with anti-DIG antibodies conjugated with alkaline phosphatase (AP) (Roche Applied Science, Indianapolis, IN). The AP activity was localized and signal was detected using NBT (0.25 mg/ml) and BCIP (0.125 mg/ml) (Roche Applied Science, Indianapolis, IN) as substrates.

For immunohistochemistry, eyecups were prepared as described above, fixed in 2% formaldehyde in 1 X PBS for 4 hours on ice, washed in 1 X PBS, cryoprotected in 30% sucrose in 1 X PBS, and embedded in Tissue-Tek O.C.T compound (Sakura Finetek USA, Torrance, CA). 10-μm cryostat sections were washed with 1 X PBS, blocked with 5% normal goat serum, 5% BSA, 0.1% fish gelatin, 0.1% Triton X-100 and 0.05% Tween 20 in 1 X PBS (blocking buffer) for 1 hour at room temperature, and then incubated with rabbit anti-Aplp2 primary antibodies (D2-II, dilution 1:1,000) [46] in blocking buffer overnight at 4°C. The sections were then washed with 0.2% Triton X-100 in 1 X PBS (PBT) and incubated with Alexa-488-conjugated donkey anti-rabbit secondary antibodies (1:500, Life Technologies, Grand Island, NY) in blocking buffer for 2 hours at room temperature. After sections were washed in PBT, they were incubated with sheep anti-Chx10 (1:200, Abcam, Cambridge, MA), or rabbit anti-Pax6 (1:1,000, Abcam, Cambridge, MA), or rabbit anti-GABA (1:100, EMD Millipore, Billerica, MA), or rabbit anti-Glycine (1:100, EMD Millipore, Billerica, MA) primary antibodies overnight (48 hours for anti-GABA and anti-Glycine antibodies) at 4°C; followed by the washes in

PBT and incubation with Alexa-594-conjugated donkey anti-sheep (1:500, Life Technologies, Grand Island, NY) or donkey anti-rabbit (1:500, Life Technologies, Grand Island, NY) secondary antibodies in blocking buffer for 2 hours at room temperature. The slides were then again washed in PBT, incubated with 300 nM DAPI in 1 X PBS, and mounted in ProLong Gold anti-fade mountant (Life Technologies, Grand Island, NY). The colocalization between Aplp2 and other antigens was examined and image capture was performed using laser scanning confocal microscope Leica TCS SP5 (Leica Microsystems, Buffalo Grove, IL) and the manufacturer's software.

Supporting Information

S1 Text. The Consortium for Refractive Error and Myopia (CREAM)–membership list. (PDF)

S1 Fig. Distribution of p-values inside and outside of the *APLP2* region–CREAM dataset. The distribution of p-values was skewed towards unexpectedly low values for SNPs in the region that showed association in ALSPAC participants (hg19 chr 11:129904497–129971498) compared to the surrounding region. The distribution inside the region was significantly skewed towards lower p-values (p = 0.005; two-sample Kolmogorov-Smirnov test) and significantly different from a uniform distribution (p = 0.001; two-sample Kolmogorov-Smirnov test). (**A**) Schematic diagram of the two regions in which the distribution of p-values was compared: i) the region where a strong association between SNP genotypes and refractive error was observed in the ALSPAC cohort (green shading); and ii) the surrounding region. (**B**) Distribution of p-values for SNPs within the region showing association in ALSPAC cohort. (**C**) Distribution of p-values for SNPs in the surrounding region. (TIF)

S2 Fig. Expression of *Aplp2* in the inner retina–immunohistochemistry. In the inner nuclear layer of the retina, *Aplp2* was expressed in the bipolar cells and glycinergic amacrines. (**Top panel**) Co-localization of Aplp2 and Chx10 demonstrating expression of *Aplp2* in the bipolar cells. Magenta arrows, Aplp2- and Chx10-positive bipolar cells; white arrows, Aplp2-positive Chx10-negative cell. (**Second and third panels**) Co-localization of Aplp2 and Pax6 demonstrating expression of *Aplp2* in the amacrine cells. Magenta arrows, Aplp2-positive Pax6-positive amacrine cells; white arrows, Aplp2-negative Pax6-positive amacrine cells. (**Fourth panel**) Co-localization of Aplp2 and glycine demonstrating expression of *Aplp2* in the glycinergic amacrines. Magenta arrows, Aplp2-positive glycine-positive amacrine cells. (**Bottom panel**) Co-localization of Aplp2 and GABA demonstrating lack of *Aplp2* expression in the GABAergic amacrines. Magenta arrows, Aplp2-negative GABA-positive amacrine cell; white arrows, Aplp2-positive GABA-negative (glycinergic) amacrine cell. (TIF)

S1 Table. Gene set enrichment analysis–correlation with the depth of the vitreous chamber. (DOCX)

S2 Table. Refractive error "growth trajectory" analysis in ALSPAC subjects. Model excluding time reading term (n = 5,200). (DOCX)

S3 Table. Refractive error "growth trajectory" analysis in ALSPAC subjects. Model excluding SNP term (n = 4,461). (DOCX)

S4 Table. Refractive error "growth trajectory" analysis in ALSPAC subjects. Full model (n = 4,461).
(DOCX)

S5 Table. Refractive error "growth trajectory" analysis in ALSPAC subjects. Model restricted to time reading "Low" subset (n = 2,775).
(DOCX)

S6 Table. Refractive error "growth trajectory" analysis in ALSPAC subjects. Model restricted to time reading "High" subset (n = 1,686).
(DOCX)

S7 Table. Logistic regression model for myopia at age 15½ years in ALSPAC subjects. Time reading ("Low" versus "High") (n = 3,312). Without interaction term.
(DOCX)

S8 Table. Logistic regression model for myopia at age 15½ years in ALSPAC subjects. Time reading ("Low" versus "High") (n = 3,312). With interaction term.
(DOCX)

S9 Table. Linear regression model for refractive error at age 15½ years in ALSPAC subjects. Time reading ("Low" versus "High") (n = 3,312).
(DOCX)

S10 Table. Linear regression model for refractive error at age 15½ years in ALSPAC subjects. Time reading ("Low" versus "High") (n = 3,312).
(DOCX)

S11 Table. Linear regression model for refractive error at age 15½ years in ALSPAC subjects. Time outdoors ("Low" versus "High") (n = 3,329).
(DOCX)

S12 Table. Linear regression model for refractive error at age 15½ years in ALSPAC subjects. Time outdoors ("Low" versus "High") (n = 3,329).
(DOCX)

S13 Table. Mouse visual acuity and contrast sensitivity data.
(XLSX)

Acknowledgments

Author Contributions

Conceived and designed the experiments: AVT TVT JAG PGH CW. Performed the experiments: AVT TVT JAG VJMV PGH PKS AK CW. Analyzed the data: AVT TVT JAG VJMV PGH RW CW. Contributed reagents/materials/analysis tools: GT. Wrote the paper: AVT TVT JAG VJMV PGH RW PKS AK GT CW.

References

1. Oyster CW (1999) The human eye: structure and function. Sunderland, MA: Sinauer Associates.

2. Wallman J, Winawer J (2004) Homeostasis of eye growth and the question of myopia. Neuron 43: 447–468. PMID: 15312645

3. Pararajasegaram R (1999) VISION 2020-the right to sight: from strategies to action. Am J Ophthalmol 128: 359–360. PMID: 10511033

4. Vitale S, Ellwein L, Cotch MF, Ferris FL 3rd, Sperduto R (2008) Prevalence of refractive error in the United States, 1999–2004. Arch Ophthalmol 126: 1111–1119. doi: 10.1001/archopht.126.8.1111 PMID: 18695106

5. Lin LL, Shih YF, Hsiao CK, Chen CJ (2004) Prevalence of myopia in Taiwanese schoolchildren: 1983 to 2000. Ann Acad Med Singapore 33: 27–33.

6. Lam CS, Goldschmidt E, Edwards MH (2004) Prevalence of myopia in local and international schools in Hong Kong. Optom Vis Sci 81: 317–322. PMID: 15181356

7. Pesudovs K, Garamendi E, Elliott DB (2006) A quality of life comparison of people wearing spectacles or contact lenses or having undergone refractive surgery. J Refract Surg 22: 19–27. PMID: 16447932

8. Rose K, Harper R, Tromans C, Waterman C, Goldberg D, et al. (2000) Quality of life in myopia. Br J Ophthalmol 84: 1031–1034. PMID: 10966960

9. Takashima T, Yokoyama T, Futagami S, Ohno-Matsui K, Tanaka H, et al. (2001) The quality of life in patients with pathologic myopia. Jpn J Ophthalmol 45: 84–92. PMID: 11163050

10. Alexander LJ (1994) Primary care of the posterior segment. Connecticut: Appleton & Lange.

11. Saw SM, Gazzard G, Shih-Yen EC, Chua WH (2005) Myopia and associated pathological complications. Ophthalmic Physiol Opt 25: 381–391. PMID: 16101943

12. Flitcroft DI (2012) The complex interactions of retinal, optical and environmental factors in myopia aetiology. Prog Retin Eye Res 31: 622–660. doi: 10.1016/j.preteyeres.2012.06.004 PMID: 22772022

13. Pizzarello L, Abiose A, Ffytche T, Duerksen R, Thulasiraj R, et al. (2004) VISION 2020: The Right to Sight: a global initiative to eliminate avoidable blindness. Arch Ophthalmol 122: 615–620. PMID: 15078680

14. Morgan IG (2003) The biological basis of myopic refractive error. Clin Exp Optom 86: 276–288. PMID: 14558849

15. Young TL (2009) Molecular genetics of human myopia: an update. Optom Vis Sci 86: E8–E22. doi: 10.1097/OPX.0b013e3181940655 PMID: 19104467

16. Baird PN, Schache M, Dirani M (2010) The GEnes in Myopia (GEM) study in understanding the aetiology of refractive errors. Prog Retin Eye Res 29: 520–542. doi: 10.1016/j.preteyeres.2010.05.004 PMID: 20576483

17. Wojciechowski R (2011) Nature and nurture: the complex genetics of myopia and refractive error. Clin Genet 79: 301–320. doi: 10.1111/j.1399-0004.2010.01592.x PMID: 21155761

18. Verhoeven VJ, Buitendijk GH, Consortium for Refractive E, Myopia, Rivadeneira F, et al. (2013) Education influences the role of genetics in myopia. Eur J Epidemiol 28: 973–980. doi: 10.1007/s10654-013-9856-1 PMID: 24142238

19. Dirani M, Chamberlain M, Shekar SN, Islam AF, Garoufalis P, et al. (2006) Heritability of refractive error and ocular biometrics: the Genes in Myopia (GEM) twin study. Invest Ophthalmol Vis Sci 47: 4756–4761. PMID: 17065484

20. Lopes MC, Andrew T, Carbonaro F, Spector TD, Hammond CJ (2009) Estimating heritability and shared environmental effects for refractive error in twin and family studies. Invest Ophthalmol Vis Sci 50: 126–131. doi: 10.1167/iovs.08-2385 PMID: 18757506

21. Peet JA, Cotch MF, Wojciechowski R, Bailey-Wilson JE, Stambolian D (2007) Heritability and familial aggregation of refractive error in the Old Order Amish. Invest Ophthalmol Vis Sci 48: 4002–4006. PMID: 17724179

22. Klein AP, Suktitipat B, Duggal P, Lee KE, Klein R, et al. (2009) Heritability analysis of spherical equivalent, axial length, corneal curvature, and anterior chamber depth in the Beaver Dam Eye Study. Arch Ophthalmol 127: 649–655. doi: 10.1001/archophthalmol.2009.61 PMID: 19433716

23. Chen CY, Scurrah KJ, Stankovich J, Garoufalis P, Dirani M, et al. (2007) Heritability and shared environment estimates for myopia and associated ocular biometric traits: the Genes in Myopia (GEM) family study. Hum Genet 121: 511–520. PMID: 17205325

24. Wojciechowski R, Congdon N, Bowie H, Munoz B, Gilbert D, et al. (2005) Heritability of refractive error and familial aggregation of myopia in an elderly American population. Invest Ophthalmol Vis Sci 46: 1588–1592. PMID: 15851555

25. Solouki AM, Verhoeven VJ, van Duijn CM, Verkerk AJ, Ikram MK, et al. (2010) A genome-wide associ-ation study identifies a susceptibility locus for refractive errors and myopia at 15q14. Nat Genet 42: 897–901. doi: 10.1038/ng.663 PMID: 20835239

26. Hysi PG, Young TL, Mackey DA, Andrew T, Fernandez-Medarde A, et al. (2010) A genome-wide association study for myopia and refractive error identifies a susceptibility locus at 15q25. Nat Genet 42: 902–905. doi: 10.1038/ng.664 PMID: 20835236

27. Li Z, Qu J, Xu X, Zhou X, Zou H, et al. (2011) A genome-wide association study reveals association between common variants in an intergenic region of 4q25 and high-grade myopia in the Chinese Han population. Hum Mol Genet 20: 2861–2868. doi: 10.1093/hmg/ddr169 PMID: 21505071

28. Shi Y, Qu J, Zhang D, Zhao P, Zhang Q, et al. (2011) Genetic variants at 13q12.12 are associated with high myopia in the han chinese population. Am J Hum Genet 88: 805–813. doi: 10.1016/j.ajhg.2011.04.022 PMID: 21640322

29. Li YJ, Goh L, Khor CC, Fan Q, Yu M, et al. (2011) Genome-wide association studies reveal genetic variants in CTNND2 for high myopia in Singapore Chinese. Ophthalmology 118: 368–375. doi: 10.1016/j.ophtha.2010.06.016 PMID: 21095009

30. Verhoeven VJ, Hysi PG, Wojciechowski R, Fan Q, Guggenheim JA, et al. (2013) Genome-wide meta-analyses of multiancestry cohorts identify multiple new susceptibility loci for refractive error and myo-pia. Nat Genet 45: 314–318. doi: 10.1038/ng.2554 PMID: 23396134

31. Farbrother JE, Kirov G, Owen MJ, Pong-Wong R, Haley CS, et al. (2004) Linkage analysis of the genetic loci for high myopia on 18p, 12q, and 17q in 51 U.K. families. Invest Ophthalmol Vis Sci 45: 2879–2885. PMID: 15326098

32. Gusev A, Bhatia G, Zaitlen N, Vilhjalmsson BJ, Diogo D, et al. (2013) Quantifying missing heritability at known GWAS loci. PLoS Genet 9: e1003993. doi: 10.1371/journal.pgen.1003993 PMID: 24385918

33. Manolio TA, Collins FS, Cox NJ, Goldstein DB, Hindorff LA, et al. (2009) Finding the missing heritabil-ity of complex diseases. Nature 461: 747–753. doi: 10.1038/nature08494 PMID: 19812666

34. Eyre-Walker A (2010) Evolution in health and medicine Sackler colloquium: Genetic architecture of a complex trait and its implications for fitness and genome-wide association studies. Proc Natl Acad Sci U S A 107 Suppl 1: 1752–1756. doi: 10.1073/pnas.0906182107 PMID: 20133822

35. Park JH, Gail MH, Weinberg CR, Carroll RJ, Chung CC, et al. (2011) Distribution of allele frequencies and effect sizes and their interrelationships for common genetic susceptibility variants. Proc Natl Acad Sci U S A 108: 18026–18031. doi: 10.1073/pnas.1114759108 PMID: 22003128

36. Lassek M, Weingarten J, Einsfelder U, Brendel P, Muller U, et al. (2013) Amyloid precursor proteins are constituents of the presynaptic active zone. J Neurochem 127: 48–56. doi: 10.1111/jnc.12358 PMID: 23815291

37. Zhang X, Herrmann U, Weyer SW, Both M, Muller UC, et al. (2013) Hippocampal network oscillations in APP/APLP2-deficient mice. PLoS One 8: e61198. doi: 10.1371/journal.pone.0061198 PMID: 23585881

38. Korte M, Herrmann U, Zhang X, Draguhn A (2012) The role of APP and APLP for synaptic transmis-sion, plasticity, and network function: lessons from genetic mouse models. Exp Brain Res 217: 435–440. doi: 10.1007/s00221-011-2894-6 PMID: 22006270

39. Weyer SW, Klevanski M, Delekate A, Voikar V, Aydin D, et al. (2011) APP and APLP2 are essential at PNS and CNS synapses for transmission, spatial learning and LTP. EMBO J 30: 2266–2280. doi: 10.1038/emboj.2011.119 PMID: 21522131

40. Schrenk-Siemens K, Perez-Alcala S, Richter J, Lacroix E, Rahuel J, et al. (2008) Embryonic stem cell-derived neurons as a cellular system to study gene function: lack of amyloid precursor proteins APP and APLP2 leads to defective synaptic transmission. Stem Cells 26: 2153–2163. doi: 10.1634/stemcells.2008-0010 PMID: 18535156

41. Herard AS, Besret L, Dubois A, Dauguet J, Delzescaux T, et al. (2006) siRNA targeted against amy-loid precursor protein impairs synaptic activity in vivo. Neurobiol Aging 27: 1740–1750. PMID: 16337035

42. Yang G, Gong YD, Gong K, Jiang WL, Kwon E, et al. (2005) Reduced synaptic vesicle density and active zone size in mice lacking amyloid precursor protein (APP) and APP-like protein 2. Neurosci Lett 384: 66–71. PMID: 15919150

43. Wang P, Yang G, Mosier DR, Chang P, Zaidi T, et al. (2005) Defective neuromuscular synapses in mice lacking amyloid precursor protein (APP) and APP-Like protein 2. J Neurosci 25: 1219–1225. PMID: 15689559

44. Leach R, Ko M, Krawetz SA (1999) Assignment of amyloid-precursor-like protein 2 gene (APLP2) to 11q24 by fluorescent in situ hybridization. Cytogenet Cell Genet 87: 215–216. PMID: 10702673

45. von Koch CS, Zheng H, Chen H, Trumbauer M, Thinakaran G, et al. (1997) Generation of APLP2 KO mice and early postnatal lethality in APLP2/APP double KO mice. Neurobiol Aging 18: 661–669. PMID: 9461064

46. Thinakaran G, Kitt CA, Roskams AJ, Slunt HH, Masliah E, et al. (1995) Distribution of an APP homolog, APLP2, in the mouse olfactory system: a potential role for APLP2 in axogenesis. J Neurosci 15: 6314–6326. PMID: 7472397

47. von Koch CS, Lahiri DK, Mammen AL, Copeland NG, Gilbert DJ, et al. (1995) The mouse APLP2 gene. Chromosomal localization and promoter characterization. J Biol Chem 270: 25475–25480. PMID: 7592716

48. Sandbrink R, Masters CL, Beyreuther K (1994) Complete nucleotide and deduced amino acid sequence of rat amyloid protein precursor-like protein 2 (APLP2/APPH): two amino acids length difference to human and murine homologues. Biochim Biophys Acta 1219: 167–170. PMID: 8086458

49. von der Kammer H, Loffler C, Hanes J, Klaudiny J, Scheit KH, et al. (1994) The gene for the amyloid precursor-like protein APLP2 is assigned to human chromosome 11q23-q25. Genomics 20: 308–311. PMID: 8020984

50. Wasco W, Gurubhagavatula S, Paradis MD, Romano DM, Sisodia SS, et al. (1993) Isolation and characterization of APLP2 encoding a homologue of the Alzheimer's associated amyloid beta protein precursor. Nat Genet 5: 95–100. PMID: 8220435

51. Cousins SL, Dai W, Stephenson FA (2015) APLP1 and APLP2, members of the APP family of proteins, behave similarly to APP in that they associate with NMDA receptors and enhance NMDA receptor surface expression. J Neurochem.

52. Aydin D, Weyer SW, Muller UC (2012) Functions of the APP gene family in the nervous system: insights from mouse models. Exp Brain Res 217: 423–434. doi: 10.1007/s00221-011-2861-2 PMID: 21931985

53. Tkatchenko AV, Walsh PA, Tkatchenko TV, Gustincich S, Raviola E (2006) Form deprivation modulates retinal neurogenesis in primate experimental myopia. Proc Natl Acad Sci U S A 103: 4681–4686. PMID: 16537371

54. Subramanian A, Kuehn H, Gould J, Tamayo P, Mesirov JP (2007) GSEA-P: a desktop application for Gene Set Enrichment Analysis. Bioinformatics 23: 3251–3253. PMID: 17644558

55. Subramanian A, Tamayo P, Mootha VK, Mukherjee S, Ebert BL, et al. (2005) Gene set enrichment analysis: a knowledge-based approach for interpreting genome-wide expression profiles. Proc Natl Acad Sci U S A 102: 15545–15550. PMID: 16199517

56. Wachtmeister L (1998) Oscillatory potentials in the retina: what do they reveal. Prog Retin Eye Res 17: 485–521. PMID: 9777648

57. Dong CJ, Agey P, Hare WA (2004) Origins of the electroretinogram oscillatory potentials in the rabbit retina. Vis Neurosci 21: 533–543. PMID: 15579219

58. Frumkes TE, Nelson R, Pflug R (1995) Functional role of GABA in cat retina: II. Effects of GABAA antagonists. Vis Neurosci 12: 651–661. PMID: 8527367

59. Green DG, Kapousta-Bruneau NV (1999) A dissection of the electroretinogram from the isolated rat retina with microelectrodes and drugs. Vis Neurosci 16: 727–741. PMID: 10431921

60. Hood DC, Birch DG (1996) Beta wave of the scotopic (rod) electroretinogram as a measure of the activity of human on-bipolar cells. J Opt Soc Am A Opt Image Sci Vis 13: 623–633. PMID: 8627419

61. Sharma S, Ball SL, Peachey NS (2005) Pharmacological studies of the mouse cone electroretinogram. Vis Neurosci 22: 631–636. PMID: 16332274

62. Sieving PA, Murayama K, Naarendorp F (1994) Push-pull model of the primate photopic electroretinogram: a role for hyperpolarizing neurons in shaping the b-wave. Vis Neurosci 11: 519–532. PMID: 8038126

63. Kapousta-Bruneau NV (2000) Opposite effects of GABA(A) and GABA(C) receptor antagonists on the b-wave of ERG recorded from the isolated rat retina. Vision Res 40: 1653–1665. PMID: 10814754

64. Dong CJ, Hare WA (2002) GABAc feedback pathway modulates the amplitude and kinetics of ERG b-wave in a mammalian retina in vivo. Vision Res 42: 1081–1087. PMID: 11997047

65. Dong CJ, Hare WA (2000) Contribution to the kinetics and amplitude of the electroretinogram b-wave by third-order retinal neurons in the rabbit retina. Vision Res 40: 579–589. PMID: 10824262

66. Lewis A, Wilson N, Stearns G, Johnson N, Nelson R, et al. (2011) Celsr3 is required for normal development of GABA circuits in the inner retina. PLoS Genet 7: e1002239. doi: 10.1371/journal.pgen.1002239 PMID: 21852962

67. Young TL, Ronan SM, Drahozal LA, Wildenberg SC, Alvear AB, et al. (1998) Evidence that a locus for familial high myopia maps to chromosome 18p. Am J Hum Genet 63: 109–119. PMID: 9634508

68. Young TL, Ronan SM, Alvear AB, Wildenberg SC, Oetting WS, et al. (1998) A second locus for familial high myopia maps to chromosome 12q. Am J Hum Genet 63: 1419–1424. PMID: 9792869

69. Naiglin L, Gazagne C, Dallongeville F, Thalamas C, Idder A, et al. (2002) A genome wide scan for familial high myopia suggests a novel locus on chromosome 7q36. J Med Genet 39: 118–124. PMID: 11836361

70. Lam DS, Tam PO, Fan DS, Baum L, Leung YF, et al. (2003) Familial high myopia linkage to chromosome 18p. Ophthalmologica 217: 115–118. PMID: 12592049

71. Paluru P, Ronan SM, Heon E, Devoto M, Wildenberg SC, et al. (2003) New locus for autosomal dominant high myopia maps to the long arm of chromosome 17. Invest Ophthalmol Vis Sci 44: 1830–1836. PMID: 12714612

72. Stambolian D, Ibay G, Reider L, Dana D, Moy C, et al. (2004) Genomewide linkage scan for myopia susceptibility loci among Ashkenazi Jewish families shows evidence of linkage on chromosome 22q12. Am J Hum Genet 75: 448–459. PMID: 15273935

73. Zhang Q, Guo X, Xiao X, Jia X, Li S, et al. (2005) A new locus for autosomal dominant high myopia maps to 4q22-q27 between D4S1578 and D4S1612. Mol Vis 11: 554–560. PMID: 16052171

74. Paluru PC, Nallasamy S, Devoto M, Rappaport EF, Young TL (2005) Identification of a novel locus on 2q for autosomal dominant high-grade myopia. Invest Ophthalmol Vis Sci 46: 2300–2307. PMID: 15980214

75. Stambolian D, Ciner EB, Reider LC, Moy C, Dana D, et al. (2005) Genome-wide scan for myopia in the Old Order Amish. Am J Ophthalmol 140: 469–476. PMID: 16084785

76. Zhang Q, Guo X, Xiao X, Jia X, Li S, et al. (2006) Novel locus for X linked recessive high myopia maps to Xq23-q25 but outside MYP1. J Med Genet 43: e20. PMID: 16648373

77. Nallasamy S, Paluru PC, Devoto M, Wasserman NF, Zhou J, et al. (2007) Genetic linkage study of high-grade myopia in a Hutterite population from South Dakota. Mol Vis 13: 229–236. PMID: 17327828

78. Yu ZQ, Li YB, Huang CX, Chu RY, Hu DN, et al. (2007) [A genome-wide screening for pathological myopia suggests a novel locus on chromosome 15q12–13]. Zhonghua Yan Ke Za Zhi 43: 233–238. PMID: 17605906

79. Paget S, Julia S, Vitezica ZG, Soler V, Malecaze F, et al. (2008) Linkage analysis of high myopia susceptibility locus in 26 families. Mol Vis 14: 2566–2574. PMID: 19122830

80. Ciner E, Wojciechowski R, Ibay G, Bailey-Wilson JE, Stambolian D (2008) Genomewide scan of ocular refraction in African-American families shows significant linkage to chromosome 7p15. Genet Epidemiol 32: 454–463. doi: 10.1002/gepi.20318 PMID: 18293391

81. Lam CY, Tam PO, Fan DS, Fan BJ, Wang DY, et al. (2008) A genome-wide scan maps a novel high myopia locus to 5p15. Invest Ophthalmol Vis Sci 49: 3768–3778. doi: 10.1167/iovs.07-1126 PMID: 18421076

82. Schache M, Chen CY, Pertile KK, Richardson AJ, Dirani M, et al. (2009) Fine mapping linkage analysis identifies a novel susceptibility locus for myopia on chromosome 2q37 adjacent to but not overlapping MYP12. Mol Vis 15: 722–730. PMID: 19365569

83. Yang Z, Xiao X, Li S, Zhang Q (2009) Clinical and linkage study on a consanguineous Chinese family with autosomal recessive high myopia. Mol Vis 15: 312–318. PMID: 19204786

84. Nishizaki R, Ota M, Inoko H, Meguro A, Shiota T, et al. (2009) New susceptibility locus for high myopia is linked to the uromodulin-like 1 (UMODL1) gene region on chromosome 21q22.3. Eye (Lond) 23: 222–229.

85. Ciner E, Ibay G, Wojciechowski R, Dana D, Holmes TN, et al. (2009) Genome-wide scan of African-American and white families for linkage to myopia. Am J Ophthalmol 147: 512–517 e512. doi: 10.1016/j.ajo.2008.09.004 PMID: 19026404

86. Li YJ, Guggenheim JA, Bulusu A, Metlapally R, Abbott D, et al. (2009) An international collaborative family-based whole-genome linkage scan for high-grade myopia. Invest Ophthalmol Vis Sci 50: 3116–3127. doi: 10.1167/iovs.08-2781 PMID: 19324860

87. Nakanishi H, Yamada R, Gotoh N, Hayashi H, Yamashiro K, et al. (2009) A genome-wide association analysis identified a novel susceptible locus for pathological myopia at 11q24.1. PLoS Genet 5: e1000660. doi: 10.1371/journal.pgen.1000660 PMID: 19779542

88. Ma JH, Shen SH, Zhang GW, Zhao DS, Xu C, et al. (2010) Identification of a locus for autosomal dominant high myopia on chromosome 5p13.3-p15.1 in a Chinese family. Mol Vis 16: 2043–2054. PMID: 21042559

89. Kiefer AK, Tung JY, Do CB, Hinds DA, Mountain JL, et al. (2013) Genome-wide analysis points to roles for extracellular matrix remodeling, the visual cycle, and neuronal development in myopia. PLoS Genet 9: e1003299. doi: 10.1371/journal.pgen.1003299 PMID: 23468642

90. Lango Allen H, Estrada K, Lettre G, Berndt SI, Weedon MN, et al. (2010) Hundreds of variants clustered in genomic loci and biological pathways affect human height. Nature 467: 832–838. doi: 10.1038/nature09410 PMID: 20881960

91. Hammond CJ, Snieder H, Gilbert CE, Spector TD (2001) Genes and environment in refractive error: the twin eye study. Invest Ophthalmol Vis Sci 42: 1232–1236. PMID: 11328732

92. Lyhne N, Sjolie AK, Kyvik KO, Green A (2001) The importance of genes and environment for ocular refraction and its determiners: a population based study among 20–45 year old twins. Br J Ophthalmol 85: 1470–1476. PMID: 11734523

93. Hammond CJ, Andrew T, Mak YT, Spector TD (2004) A susceptibility locus for myopia in the normal population is linked to the PAX6 gene region on chromosome 11: a genomewide scan of dizygotic twins. Am J Hum Genet 75: 294–304. PMID: 15307048

94. Slunt HH, Thinakaran G, Von Koch C, Lo AC, Tanzi RE, et al. (1994) Expression of a ubiquitous, cross-reactive homologue of the mouse beta-amyloid precursor protein (APP). J Biol Chem 269: 2637–2644. PMID: 8300594

95. Heber S, Herms J, Gajic V, Hainfellner J, Aguzzi A, et al. (2000) Mice with combined gene knock-outs reveal essential and partially redundant functions of amyloid precursor protein family members. J Neurosci 20: 7951–7963. PMID: 11050115

96. Soba P, Eggert S, Wagner K, Zentgraf H, Siehl K, et al. (2005) Homo- and heterodimerization of APP family members promotes intercellular adhesion. EMBO J 24: 3624–3634. PMID: 16193067

97. Herms J, Anliker B, Heber S, Ring S, Fuhrmann M, et al. (2004) Cortical dysplasia resembling human type 2 lissencephaly in mice lacking all three APP family members. EMBO J 23: 4106–4115. PMID: 15385965

98. Stone RA, Laties AM, Raviola E, Wiesel TN (1988) Increase in retinal vasoactive intestinal polypeptide after eyelid fusion in primates. Proc Natl Acad Sci U S A 85: 257–260. PMID: 2448769

99. Seltner RL, Stell WK (1995) The effect of vasoactive intestinal peptide on development of form deprivation myopia in the chick: a pharmacological and immunocytochemical study. Vision Res 35: 1265–1270. PMID: 7610586

100. Fischer AJ, Seltner RL, Stell WK (1997) N-methyl-D-aspartate-induced excitotoxicity causes myopia in hatched chicks. Can J Ophthalmol 32: 373–377. PMID: 9363340

101. Fischer AJ, McGuire JJ, Schaeffel F, Stell WK (1999) Light- and focus-dependent expression of the transcription factor ZENK in the chick retina. Nat Neurosci 2: 706–712. PMID: 10412059

102. Feldkaemper MP, Schaeffel F (2002) Evidence for a potential role of glucagon during eye growth regulation in chicks. Vis Neurosci 19: 755–766. PMID: 12688670

103. Zhong X, Ge J, Smith EL 3rd, Stell WK (2004) Image defocus modulates activity of bipolar and amacrine cells in macaque retina. Invest Ophthalmol Vis Sci 45: 2065–2074. PMID: 15223778

104. Vessey KA, Lencses KA, Rushforth DA, Hruby VJ, Stell WK (2005) Glucagon receptor agonists and antagonists affect the growth of the chick eye: a role for glucagonergic regulation of emmetropization? Invest Ophthalmol Vis Sci 46: 3922–3931. PMID: 16249465

105. Chen JC, Brown B, Schmid KL (2006) Evaluation of inner retinal function in myopia using oscillatory potentials of the multifocal electroretinogram. Vision Res 46: 4096–4103. PMID: 17010409

106. Mathis U, Schaeffel F (2007) Glucagon-related peptides in the mouse retina and the effects of deprivation of form vision. Graefes Arch Clin Exp Ophthalmol 245: 267–275. PMID: 16741711

107. Feldkaemper MP, Neacsu I, Schaeffel F (2009) Insulin acts as a powerful stimulator of axial myopia in chicks. Invest Ophthalmol Vis Sci 50: 13–23. doi: 10.1167/iovs.08-1702 PMID: 18599564

108. Ashby R, Kozulin P, Megaw PL, Morgan IG (2010) Alterations in ZENK and glucagon RNA transcript expression during increased ocular growth in chickens. Mol Vis 16: 639–649. PMID: 20405027

109. Wassle H, Heinze L, Ivanova E, Majumdar S, Weiss J, et al. (2009) Glycinergic transmission in the Mammalian retina. Front Mol Neurosci 2: 6. doi: 10.3389/neuro.02.006.2009 PMID: 19924257

110. Werblin FS (2010) Six different roles for crossover inhibition in the retina: correcting the nonlinearities of synaptic transmission. Vis Neurosci 27: 1–8. doi: 10.1017/S0952523810000076 PMID: 20392301

111. Russell TL, Werblin FS (2010) Retinal synaptic pathways underlying the response of the rabbit local edge detector. J Neurophysiol 103: 2757–2769. doi: 10.1152/jn.00987.2009 PMID: 20457864

112. Zhang C, McCall MA (2012) Receptor targets of amacrine cells. Vis Neurosci 29: 11–29. doi: 10.1017/S0952523812000028 PMID: 22310370

113. Buldyrev I, Taylor WR (2013) Inhibitory mechanisms that generate centre and surround properties in ON and OFF brisk-sustained ganglion cells in the rabbit retina. J Physiol 591: 303–325. doi: 10.1113/jphysiol.2012.243113 PMID: 23045347

114. Buldyrev I, Puthussery T, Taylor WR (2012) Synaptic pathways that shape the excitatory drive in an OFF retinal ganglion cell. J Neurophysiol 107: 1795–1807. doi: 10.1152/jn.00924.2011 PMID: 22205648

115. Venkataramani S, Van Wyk M, Buldyrev I, Sivyer B, Vaney DI, et al. (2014) Distinct roles for inhibition in spatial and temporal tuning of local edge detectors in the rabbit retina. PLoS One 9: e88560. doi: 10.1371/journal.pone.0088560 PMID: 24586343

116. Gwiazda J, Thorn F, Bauer J, Held R (1993) Myopic children show insufficient accommodative response to blur. Invest Ophthalmol Vis Sci 34: 690–694. PMID: 8449687

117. Seidemann A, Schaeffel F (2003) An evaluation of the lag of accommodation using photorefraction. Vision Res 43: 419–430. PMID: 12535999

118. Smith EL 3rd, Hung LF, Huang J (2009) Relative peripheral hyperopic defocus alters central refractive development in infant monkeys. Vision Res 49: 2386–2392. doi: 10.1016/j.visres.2009.07.011 PMID: 19632261

119. Boyd A, Golding J, Macleod J, Lawlor DA, Fraser A, et al. (2013) Cohort Profile: the 'children of the 90s'—the index offspring of the Avon Longitudinal Study of Parents and Children. Int J Epidemiol 42: 111–127. doi: 10.1093/ije/dys064 PMID: 22507743

120. Guggenheim JA, Northstone K, McMahon G, Ness AR, Deere K, et al. (2012) Time outdoors and physical activity as predictors of incident myopia in childhood: a prospective cohort study. Invest Ophthalmol Vis Sci 53: 2856–2865. doi: 10.1167/iovs.11-9091 PMID: 22491403

121. Guggenheim JA, Zhou X, Evans DM, Timpson NJ, McMahon G, et al. (2013) Coordinated genetic scaling of the human eye: shared determination of axial eye length and corneal curvature. Invest Ophthalmol Vis Sci 54: 1715–1721. doi: 10.1167/iovs.12-10560 PMID: 23385790

122. Li Y, Willer CJ, Ding J, Scheet P, Abecasis GR (2010) MaCH: using sequence and genotype data to estimate haplotypes and unobserved genotypes. Genet Epidemiol 34: 816–834. doi: 10.1002/gepi.20533 PMID: 21058334

123. Mattapallil MJ, Wawrousek EF, Chan CC, Zhao H, Roychoudhury J, et al. (2012) The Rd8 Mutation of the Crb1 Gene Is Present in Vendor Lines of C57BL/6N Mice and Embryonic Stem Cells, and Confounds Ocular Induced Mutant Phenotypes. Invest Ophthalmol Vis Sci 53: 2921–2927. doi: 10.1167/iovs.12-9662 PMID: 22447858

124. Tkatchenko TV, Shen Y, Tkatchenko AV (2010) Analysis of postnatal eye development in the mouse with high-resolution small animal magnetic resonance imaging. Invest Ophthalmol Vis Sci 51: 21–27. doi: 10.1167/iovs.08-2767 PMID: 19661239

125. Tkatchenko AV, Shen Y, Tkatchenko TV (2012) Genetic background modulates refractive eye development and susceptibility to myopia in the mouse. Invest Ophthalmol Vis Sci 53: E-Abstract 3465.

126. Tkatchenko TV, Shen Y, Braun RD, Bawa G, Kumar P, et al. (2013) Photopic visual input is necessary for emmetropization in mice. Exp Eye Res 115C: 87–95.

127. Tkatchenko TV, Tkatchenko AV (2010) Ketamine-xylazine anesthesia causes hyperopic refractive shift in mice. J Neurosci Methods 193: 67–71. doi: 10.1016/j.jneumeth.2010.07.036 PMID: 20813132

128. Parssinen O, Lyyra AL (1993) Myopia and myopic progression among schoolchildren: a three-year follow-up study. Invest Ophthalmol Vis Sci 34: 2794–2802. PMID: 8344801

129. Goss DA (2000) Nearwork and myopia. Lancet 356: 1456–1457. PMID: 11081523

130. Hepsen IF, Evereklioglu C, Bayramlar H (2001) The effect of reading and near-work on the development of myopia in emmetropic boys: a prospective, controlled, three-year follow-up study. Vision Res 41: 2511–2520. PMID: 11483181

131. Saw SM, Chua WH, Hong CY, Wu HM, Chan WY, et al. (2002) Nearwork in early-onset myopia. Invest Ophthalmol Vis Sci 43: 332–339. PMID: 11818374

132. Gwiazda J, Bauer J, Thorn F, Held R (1995) A dynamic relationship between myopia and blur-driven accommodation in school-aged children. Vision Res 35: 1299–1304. PMID: 7610590

133. Abbott ML, Schmid KL, Strang NC (1998) Differences in the accommodation stimulus response curves of adult myopes and emmetropes. Ophthalmic Physiol Opt 18: 13–20. PMID: 9666906

134. Charman WN (1999) Near vision, lags of accommodation and myopia. Ophthalmic Physiol Opt 19: 126–133. PMID: 10615448

135. Gwiazda JE, Hyman L, Norton TT, Hussein ME, Marsh-Tootle W, et al. (2004) Accommodation and related risk factors associated with myopia progression and their interaction with treatment in COMET children. Invest Ophthalmol Vis Sci 45: 2143–2151. PMID: 15223788

136.   Shen W, Vijayan M, Sivak JG (2005) Inducing form-deprivation myopia in fish. Invest Ophthalmol Vis Sci 46: 1797–1803. PMID: 15851585

137.   Wallman J, Turkel J, Trachtman J (1978) Extreme myopia produced by modest change in early visual experience. Science 201: 1249–1251. PMID: 694514

138.   Sherman SM, Norton TT, Casagrande VA (1977) Myopia in the lid-sutured tree shrew (Tupaia glis). Brain Res 124: 154–157. PMID: 843938

139.   Wiesel TN, Raviola E (1977) Myopia and eye enlargement after neonatal lid fusion in monkeys. Nature 266: 66–68. PMID: 402582

140.   Smith EL 3rd, Hung LF (1999) The role of optical defocus in regulating refractive development in infant monkeys. Vision Res 39: 1415–1435. PMID: 10343811

141.   Howlett MH, McFadden SA (2009) Spectacle lens compensation in the pigmented guinea pig. Vision Res 49: 219–227. doi: 10.1016/j.visres.2008.10.008 PMID: 18992765

142.   Howlett MH, McFadden SA (2006) Form-deprivation myopia in the guinea pig (Cavia porcellus). Vision Res 46: 267–283. PMID: 16139323

143.   Tkatchenko TV, Shen Y, Tkatchenko AV (2010) Mouse experimental myopia has features of primate myopia. Invest Ophthalmol Vis Sci 51: 1297–1303. doi: 10.1167/iovs.09-4153 PMID: 19875658

144.   Schaeffel F, Burkhardt E, Howland HC, Williams RW (2004) Measurement of refractive state and deprivation myopia in two strains of mice. Optom Vis Sci 81: 99–110. PMID: 15127929

145.   Prusky GT, Alam NM, Beekman S, Douglas RM (2004) Rapid quantification of adult and developing mouse spatial vision using a virtual optomotor system. Invest Ophthalmol Vis Sci 45: 4611–4616. PMID: 15557474

146.   Yang H, Wanner IB, Roper SD, Chaudhari N (1999) An optimized method for in situ hybridization with signal amplification that allows the detection of rare mRNAs. J Histochem Cytochem 47: 431–446. PMID: 10082745